PHYSICAL REVIEW D VOLUME 39, NUMBER 9 1 MAY 1989

Scattering in nuclei and QCD

Keith Kastella and George Sterman
Institute for Theoretical Physics, State University of New York at Stony Brook, Stony Brook, New York 11794-3840

Joseph Milana
Physics Department, Oregon State University, Corvallis, Oregon 97331
(Received 2 December 1988)

We argue that double scattering in nuclei can be treated perturbatively in QCD, and derive expressions for double-scattering contributions to short-distance cross sections. These cross sections are sensitive to the distribution of gluons at low x.

I. INTRODUCTION

Important atomic-number (A) dependence has long been observed in high-$P_\perp$ hadron-nucleus reactions, and more recently in lepton pair production in nuclei.[1] One plausible explanation for A dependence has been found in multiple scattering of a single parton of the projectile hadron.[2] When all these scatterings involve large momentum transfer, they may be treated as localized QCD subprocesses.[3] In the limit where one scattering is soft, however, these models require an infrared cutoff,[4] and are sensitive to nonperturbative effects.

The importance of soft scatterings over nuclear scales was pointed out in Ref. 5. Although these soft effects turn out to be higher twist,[6,7] they may still play a role because they grow with nuclear dimensions.

In the following, we study sequential multiple scattering in the context of perturbative QCD. We argue that double scattering, at least, may be treated perturbatively as a factorizing, first-nonleading-twist effect, and that to leading power in the nuclear radius (or equivalently in our approximation, $A^{1/3}$), the double-scattering cross section is determined by the distribution of gluons in a bound nucleon. In particular, we find that the leading A dependence is sensitive to the small-x behavior of the gluon distribution.[8] This is in contrast to models in which multiple scattering is treated in terms of the quark-nucleon cross section.[9] Finally, triple or higher scatterings should be suppressed by extra factors of $A^{1/3}/R_0^2Q^2$ (R_0 is the internucleon separation), which we take to be small.

When both scatterings are hard, the model of Ref. 3 (which we refer to as the "hard-scattering" model) should be adequate, and we review it in Sec. II. In Sec. III we present arguments which suggest that double hard scattering is a perturbative higher-twist effect, and that the leading noncancelling contribution involves the physical degrees of freedom of the soft gluon. Sections IV–VII describe the process of verifying this result at lowest order. Section IV describes the diagrammatic approach, in which the projectile parton is treated perturbatively, and the target nonperturbatively. We develop our approximations for the target structure in Sec. V, and analyze the projectile in Sec. VI, showing how short- and long-distance effects factorize and the leading power cancels. In Sec. VII we show that the remaining contribution involves matrix elements of the gluonic field strength. Finally, in Sec. VIII we summarize our results on soft scattering, combine them with the hard-scattering model, and discuss the interplay of nuclear structure with the gluon distribution in determining A dependence.

II. HARD-SCATTERING MODEL

In order to set the context, we briefly review the hard-scattering model[3] specialized to double scattering, and neglecting "intrinsic" transverse momentum. Consider the single-particle inclusive cross section for projectile h with momentum P_h to produce hadron h' with momentum $P_{h'}$ on nucleus A, with momentum transfer $\tilde{Q}^2=-2P_h\cdot P_{h'}$. For simplicity at high energy, we drop projectile masses in the kinematics.

The active parton, of type i from hadron h, has momentum

$$l^\mu=l^+v^\mu=x_iP_h^\mu\ , \tag{2.1}$$

where $v^\mu\equiv\delta^{\mu+}$. This parton scatters elastically into the final momentum $l'=l+Q$ after two collisions, and then fragments into the observed hadron h' with momentum fraction z, so that

$$Q^2=x_i\frac{1}{z}\tilde{Q}^2\ . \tag{2.2}$$

The parton sequentially absorbs momenta $(Q-q)^\mu$ and q^μ from the target. Our main interest will be in the "soft regions" for which $q_\perp\ll Q_\perp$ or $|Q_\perp-q_\perp|\ll Q_\perp$.

For its part, the nucleus is modeled in its rest frame as a sphere of radius $R=R_0A^{1/3}$ centered at the origin, with uniform number density $\rho=3/4\pi R_0^3$. The parton-model cross sections $h^{ij}(l;l')\equiv E'd\sigma^{i\to j}/d^3l'$ for projectile partons to make the transition $i\to j$ in flavor and $l\to l'$ in momentum on a single-nucleon target with momentum P_n are

$$h^{ij}(l;l')=\frac{1}{\pi}\frac{s}{s+u}\sum_m x_mf_{m/N}(x_m)\frac{d\sigma^{im\to jX}}{dt}\ , \tag{2.3}$$

where m labels the partons in nucleon N and $d\sigma/dt$ is a standard cross section for elastic parton-parton scattering at fixed t. The relevant invariants are

$$s=2l\cdot p_N,\quad t=-2l\cdot l'=Q^2\ ,$$
$$u=-2p_N\cdot l',\quad x_m=\frac{-t}{s+u}\ . \tag{2.4}$$

In order to obtain an expression in terms of the hadronic, rather than partonic, initial and final states, we fold in structure and fragmentation functions for h and h' with the measure

$$d(fD)\equiv dx_i f_{i/h}(x_i,\mu^2)\frac{dz}{z^2}D_{j/h'}(z,\mu^2)\ .$$

For jet cross sections, fragmentation is omitted. Since the two collisions have different momentum transfers, it is not *a priori* clear what scale μ is to be used in evaluating $f_{i/h}$ and $D_{j/h'}$, but in the next section we will argue that $\mu^2=Q^2$ is most appropriate. Fixing the momentum of the observed particle, the cross section including double scattering becomes[3]

$$\omega_{l'}\frac{d\sigma^{ik}_{\rm hard}}{d^3l'}=Ah^{ik}(l,l')+\frac{9A^{4/3}}{16\pi R_0^2}\int_0^1 dx_i f_{i/h}(x_i)\int\frac{dq^+d^2\mathbf{q}_\perp}{l^++q^+}\sum_j[h^{ij}(l,l+q)h^{jk}(l+q,l')-h^{ik}(l,l')h^{kj}(l',l+q)$$
$$-h^{ij}(l,l+q)h^{ik}(l,l')]\ . \tag{2.5}$$

Here the limits on the q^+ and Q^+ integrals are set implicitly by the requirement that x_m be less than or equal to one for each scattering. In the $A^{4/3}$ part of Eq. (2.5) the positive term describes physical double scattering into the observed state. The two negative terms describe "absorption" from the states of momentum l and $l+Q$, respectively, and are proportional to the lowest-order total cross sections at these momenta. With t-channel exchange, $h^{ij}(l;l+q)\sim\alpha_s^2(q^2)^{-2}$, so that (2.5) is ill defined when $q^2=0$ or $(Q-q)^2=0$. If we cut off the integrals in these soft regions with a parameter $t_{\rm min}$, then the strongest infrared dependence in the scattering and absorption terms, proportional to $t_{\rm min}^{-1}$, cancels, but leaves behind an uncanceled singularity proportional to $(Q_\perp^2)^{-1}\ln t_{\rm min}$ (Ref. 4).

When we analyze this problem below in perturbative QCD, a structure similar to that of (2.5) will emerge, in the form of a higher-twist effect. The $Q_\perp^{-2}\ln t_{\rm min}$ divergence will then be absorbed into a multiparton distribution, from which arises the enhanced A dependence.

III. PERTURBATIVE QCD AND THE COUPLING SCALE

In discussing double scattering from the point of view of field theory, we will rely heavily on experience drawn from the proof of factorization at leading twist.[6,7] Standard factorization theorems assert that cross sections for large momentum transfer reactions may be written as

$$d\sigma=\sum_{a,b}\int_0^1 dx_a dx_b f_{a/h}(x_a,Q^2)\omega_{ab}(x_a,x_b,Q^2)$$
$$\times f_{b/h'}(x_b,Q^2)\ . \tag{3.1}$$

This is a convolution of distributions $f_{a/h}(x_a,Q^2)$ of partons a in the colliding hadrons h and short-distance functions $\omega_{ab}(x_a,x_b,Q^2)$. The distributions $f_{a/h}$ must be determined from experiment at some energy scale Q_0^2, after which their evolution may be calculated. The short-distance functions may be calculated in perturbation theory once the distribution is specified. In lowest order, they are given by Born approximation cross sections. The parton-model cross section, Eq. (2.3), is of the factorized form. This is to be expected, since factorized cross sections are a generalization, and in some sense a justification, of parton-model cross sections.

The extension of factorization theorems to higher twist is very nontrivial. Although originally suggested for all hard-scattering processes,[10] most work in this direction has concentrated on deeply inelastic scattering.[11,12] In this case, higher-twist contributions to the cross sections may be expressed in terms of a generalization of parton distributions to several partons in a hadron. In hadron-hadron scattering, however, the situation is not so clear. Perturbation theory definitely allows nonfactoring contributions at higher twist. The failure of factorization is seen in noncancelling infrared divergences[13] at two loops in the eikonal approximation, and even at one loop[14] when finite contributions are taken into account.

An important point should be made about these explicit nonfactoring contributions. In eikonal approximation, the hard scattering is pointlike with respect to soft corrections, and, in this approximation nonfactoring contributions appear at a relative suppression of s^{-2} from the leading power, with s the invariant mass squared of the system. From a classical point of view, this is a natural result.[14] Factorization fails when the colliding hadrons may influence each others' parton distributions before the hard collision, and this can only happen to the extent that they feel each others' fields before they collide. Now in the rest frame of one hadron (A, say), the fields of the incident hadron (B) are Lorentz contracted. In fact, at any fixed time scale before or after the collision, the field strengths due to B in this frame are suppressed by a factor of order $(1-v_B^2/c^2)^2$, proportional to $(s/m_A m_B)^{-2}$. This suppression arises because the vector potential due to B is nearly gauge equivalent to zero in the rest frame of A, until the particles are right on top of each other. Proofs of factorization in quantum field theory[7] rely on the analogous feature that soft gluons exchanged between incoming hadrons are equivalent to gluons with unphysical polarizations. It is

thus not unreasonable to expect that nonfactoring contributions to pointlike scattering occur at the level of s^{-2} quite generally.

With this assumption in hand, we will argue that the leading dependence on the nuclear size in QCD is proportional to $\alpha_s(Q^2)(A^{1/3}/R_0^2Q^2)$, where R_0 is the internucleon separation. It is thus both higher twist and perturbatively computable. Contributions of this sort are associated with double scattering, and, although the momentum transfer at one of the scatterings may be small, the coupling is associated with the *hard* scattering. This might be a surprising result, because one might expect an incident parton to undergo numerous soft scatterings, and absorb numerous soft gluons, as it passes through a large nucleus. We will try to argue that—because of the presence of the hard scattering—this is not the case.

Let us begin with a discussion in the style of the parton model, working in the rest frame of the nucleus. Because of time dilation, many virtual states of the projectile particle live long enough to cross the entire nucleus. These include states in which one or more partons of the projectile possess large transverse momentum. If the total momentum transfer is low, these states do not contribute much in the amplitude, simply because they do not match up with the final state of the system. When the parton undergoes a hard scattering, however, we know that there will always be gluon radiation in the final state. This means that states in which the scattered parton takes on relatively large transverse momentum, balanced by the transverse momentum of radiated gluons, dominate the sum of states which contribute to the amplitude. This large spread in transverse momentum localizes the scattered parton at the transverse position of the hard scattering, within an uncertainty of only $1/Q^2$. Without the hard scattering, of course, it might be anywhere within the radius of the projectile hadron. Once localized, the probability for the parton to collide with partons from the nucleus is drastically reduced. The density of partons in the nucleus is proportional to R_0^{-3}, independent of R, the nuclear radius. n additional scatterings should then occur with a probability of order $[R/(Q^2R_0^3)]^n=[A^{1/3}/(R_0^2Q^2)]^n$, which is the order of the effective transverse size of the scattered parton times the number of partons per unit area in the nucleus. For large Q, an expansion in n is quite reasonable. Note that the distribution of virtual states in the incoming hadron is independent of the target only to the extent that we can ignore "initial-state" interactions which act on long time scales before the collision. In view of our comments above, this is the case perturbatively only for $n=1$. For $n\geq 2$ such initial-state interactions should be taken into account. Neglecting this effect, however, the scattered parton propagates near the light cone, in the target rest frame, and its additional interactions are suppressed, just as in deeply inelastic scattering.[11,12]

The scattered parton is also unlikely to interact with other partons from the projectile, for the same geometric reason. In particular, the projectile takes so short a time in its own rest frame to cross the nucleus that it has no time to form a pomeron, which requires long-time interactions between its partons.[15] In the following, we will try to see how this simple picture might emerge in perturbative QCD.

We begin with Fig. 1(a), working in the center-of-mass frame of the projectile hadron and a typical nucleon of the target. In the following, $s^{1/2}$ will denote their invariant mass. In Fig. 1(a), two partons of the nucleus, of momenta $p_2^\mu+q^\mu$ and $p_1^\mu-q^\mu$, scatter the projectile parton by single-gluon exchange, with momentum q^μ and $(Q-q)^\mu$. We assume that $Q^2=O(s)$, while q^μ may be quite soft. The projectile momentum is $l^\mu=l^+\delta^{\mu+}$, while

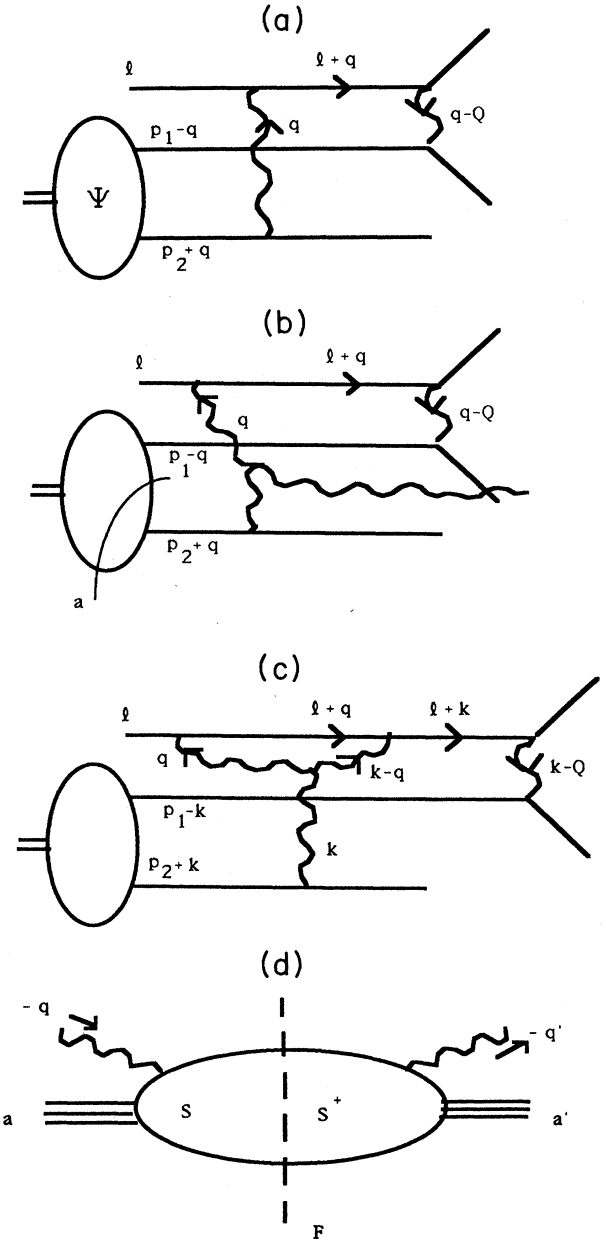

FIG. 1. (a) Lowest-order example of double scattering; (b) lowest-order example of spectator interaction; (c) spectator interaction when plus momentum flows back to the active line; (d) cut diagram generated from spectator and target poles.

p_1^μ and p_2^μ are assumed to be primarily in the minus direction. Ψ represents a hadron wave function, which in this frame is spread out in minus momentum, and is sharply peaked in plus momentum.

To discuss the role played by a soft gluon in factorization, we must first specify its plus momentum. When q^+ is positive, the parton-model picture described above emerges almost immediately. To see this, we must use our ability to deform momentum contour integrals in Feynman diagrams. Consider q^-, the minus component of the loop which flows with the arrows in the figure. In general, poles will occur near the origin in q^- only from the lines with momentum q^μ and $l^\mu+q^\mu$, the other lines and the wave function not being strongly dependent on q^- for small q^-. The relevant poles are

$$q^- = \frac{q_\perp^2 - i\epsilon}{2(l^+ + q^+)}, \quad q^- = \frac{q_\perp^2 - i\epsilon}{2q^+} . \tag{3.2}$$

Now for q^+ positive, both these poles are in the lower half-plane, and the q^- integral may be deformed so that it never comes nearer to them than $O(s^{1/2})$. Then, assuming $q_\perp$ is fixed, the gluon of momentum q^μ has a momentum characteristic of a hard parton of the nucleus along the entire q^- contour. In this case, the scattered projectile line $l^\mu+q^\mu$ is off-shell by $O(l^+q^-)=O(s)$, and there is effectively only a single hard scattering. In particular, this ensures that radiative corrections to this scattering will have scales characteristic of $\alpha_s(Q^2)$ (Ref. 16), and that the evolution of parton distributions and fragmentation functions is determined by Q^2. This is precisely analogous to the observation above that the cross section of the projectile with a parton of the nucleus is characteristic of the hard scattering.[17] We emphasize that the soft-exchange gluon q^μ plays the role of one of the target partons, and factorizes from the hard interaction.

Simple dimensional considerations, formalized in Ref. 18, show that a hard scattering involving two partons from the target (in this case, p_1 and q) is suppressed by a single factor of at least $s^{-1/2}$ from the leading behavior unless one of the target partons is an (unphysical) longitudinally polarized gluon. Contributions from such gluons, on the other hand, are familiar in leading-twist factorization arguments. They either cancel or are absorbed into the definition of the parton distribution for the hard scattering.[7] This leaves only the power-suppressed physical polarizations of the gluon. This power will become s^{-1} in the squared amplitude, and we derive the energy dependence of the parton model discussed above, now times $\alpha_s(Q^2)$.

We next consider the possibility that q^+ is negative, in which case the two poles in Eq. (3.2) will be on opposite sides of the real q^- axis. In this case, we are unable to deform the q^- contour as before, unless q^+ is so small that $q_\perp^2/q^+$ is of order $s^{-1/2}$. This is not surprising because, whenever q^+ is non-negligible, it is no longer natural to consider the gluon q^μ as a constituent of the nucleus. So, we must resort to slightly different reasoning.

We observe that in the frame we have chosen, the plus momenta in the nucleus are small, typically of order $m^2/\sqrt{s}$, with m a typical nuclear or nucleon mass scale. If q^+ is larger than this, it must flow either into the final state, as in Fig. 1(b), or back to the projectile line, as along line $k^\mu-q^\mu$ in Fig. 1(c). Let us deal with these cases in turn.

First, suppose that the plus momentum flows into the final state. In this case, the gluon of momentum q^μ acts like a spectator to the hard interaction. In particular, if we deform the q^- integral into the upper half-plane, we will cross the second pole in Eq. (3.2), whose contribution must be added to that of the deformed contour. Along the deformed contour both q and $l+q$ are far off-shell, and we may proceed as before. In the pole term, however, the q^μ line is fixed on-shell. For this term, we turn to the q^+ contour. Deforming it into the lower half-plane, we get contributions from discontinuities of the wave function, the simplest of which is the single-particle pole when $p_2^\mu+q^\mu$ is on-shell. The deformed q^+ contour, on the other hand, gives a negligible contribution, since the wave function is supposed to be a rapidly decreasing function of q^+. The discontinuities in the lower half-plane are associated with intermediate states, labeled a in Fig. 1(b), which, along with the q^2 pole, disconnect the diagram. The disconnected subdiagram represents the on-shell scattering of the gluon of momentum $-q^\mu$ with a subset of partons a from the nucleus. When we square the amplitude, these gluon scattering contributions correspond to cut diagrams of the form shown in Fig. 1(d). Such cut diagrams are contributions to $S^*(-q',a';F)S(F;-q,a)$ where $S(F;-q,a)$ is the S matrix for the process gluon $(-q^\mu)$+state $a\rightarrow$state F. Fixing the remainder of the diagram, we can sum over final-state F at a fixed order in the coupling, not forgetting the possibilities $F=(-q,a)$ and $F=(-q',a')$. The sum of all cut diagrams is then proportional to the perturbative expansion of the unitarity relation $S^\dagger S=1$, and all nonzero orders in the perturbative expansion cancel. Thus, the contributions of spectator pole terms of the type in Fig. 1(b) cancel in the cross section after the sum over final states.[7,19] This is the analog of the parton-model statement that interactions of the spectators do not affect the hard scattering.

In the second case, when the plus momentum flows back to the projectile along line $k^\mu-q^\mu$, we can treat the line k^μ as an additional parton of the target, just as above. Then gluons $-q^\mu$ and k^μ carry large plus and minus momenta, respectively, into a hard subdiagram, consisting of lines all of which are far off the mass shell [$k-q$, $l+k$, and $k-Q$ in Fig. 1(c)]. It may be useful to note here that this reasoning can easily be generalized to the ladders which build up Reggeon exchanges.[15] Our ability to deform the k^- contour destroys the strong ordering in plus and minus momenta which characterizes such a ladder. This corresponds to the parton-model statement that there is not enough time between the soft and hard scatterings to form a pomeron.

While these low-order arguments are far from all inclusive, we think they demonstrate that perturbative contributions may be expected to follow the pattern suggested by the parton model. The conclusion is that in the presence of a hard scattering, additional soft scatterings

may be treated perturbatively, even if they carry low transverse momenta. The contributions of these scatterings are always higher twist, although graph-by-graph unphysical gluon polarizations may give leading-twist effects which cancel in a sum over diagrams. The next four sections of this paper give a detailed treatment of soft scattering at lowest order. Our aim is to disentangle in this simple case the higher-twist physical soft scattering, and to verify the cancellation of the unphysical leading twist. We work to leading power in A, and this will lead to a number of simplifications. In particular, our multiple-parton distributions will reduce to products of single-nucleon distributions, as suggested in Ref. 20 in the context of deeply inelastic scattering.

IV. DIAGRAMS

We now study double scattering on a nuclear target, working at lowest order in $\alpha_s(Q^2)$ in accordance with the discussion of the previous section, but without assuming the explicit incoherence of the hard-scattering model. We will isolate the higher-twist (i.e., $Q_\perp^{-6}$) dependence in the cross section, which scales as $A^{4/3}$ in the limit that one scattering is soft. In the cross section, double scattering requires an $O(g^4(Q^2))$ interaction for the projectile. We will work at this (lowest) order for the incoming projectile, but will not assume that the target may be treated perturbatively. The contributions to the cross section at fixed $Q_\perp$ may thus be represented as in Figs. 2–4. These figures represent an amplitude and its complex conjugate, separated by a vertical line which denotes the final state. In each case $\hat{H}$ labels the "hard" scattering, at which the large momentum transfer Q^μ primarily takes place. $\hat{H}$ includes, in general, annihilation as well as gluon-exchange graphs. The target, labeled $\mathcal{T}$, is represented by a single blob, while the incoming quark l^μ, the outgoing quark $l'^\mu = l^\mu + Q^\mu$, and the soft gluons are shown explicitly. For the remainder of the paper we work in the target rest frame.

Figures 2(a) and 2(b) represent, respectively, a square of the double-scattering amplitude and the corresponding interference term. They are analogous to initial-state double-scattering and absorption contributions to Eq. (2.5). Similarly, Figs. 3(a) and 3(b) represent final-state interactions, and Fig. 4 (below) a mixture of initial and final state. Note that the (coherent) mixed case has no analog in Eq. (2.5).

In the figures, the momenta k^μ and q^μ flow between the two scatterings. If both k^μ and q^μ are hard, the two scatterings are not independent. Instead we have a higher-order correction to a single hard scattering. We shall assume in each case that k^μ is a soft momentum, while q^μ ranges from soft to hard. More detailed assumptions on the nature of $\mathcal{T}$ are discussed below, but for now we assume that k^μ connects different constituents of the nuclear state $|P\rangle$, and as a result, the k^μ integral gets contributions from a limited but finite region on the real axis whose width is set in the nucleus rest frame by the nuclear size $R = R_0 A^{1/3}$, inside of which the nuclear wave function is nonvanishing.

When $q_\perp$ and $(Q_\perp - q_\perp)$ in Figs. 2–4 are of $O(s^{1/2})$, then all projectile interactions are hard. This region of momentum space is not the source of any infrared problems in the hard-scattering model, and we will assume that in this region it is adequate. We therefore concentrate on the regions when one of the projectile interactions is soft. In the case when $\hat{H}$ in Fig. 2(a) consists of an $O(g^4)$ t-channel gluon exchange, Fig. 3(a) receives a contribution from the same graph. There is no question of double counting, however, since the transverse-momentum flow in the two contributions is different. They are related by the change of variables $q^\mu \to Q^\mu - q^\mu$. In each case, we shall require a restriction on the transverse momentum $q_\perp$, as labeled in the graph, of the form $|q_\perp| < \beta |Q_\perp|$, where β is some fraction of unity. We shall see that the ambiguity in choosing β is similar to the ambiguity in choosing the factorization scale.[21] We label this "soft" region for the ith graph as Σ_i.

With these assumptions, we may write the full contribution of soft double scattering to the cross sections as

$$d\sigma_{\text{soft}} = \sum_{i=2,3,4} d\sigma_{\text{soft}}^{(i)} , \tag{4.1}$$

where i labels the graph and where

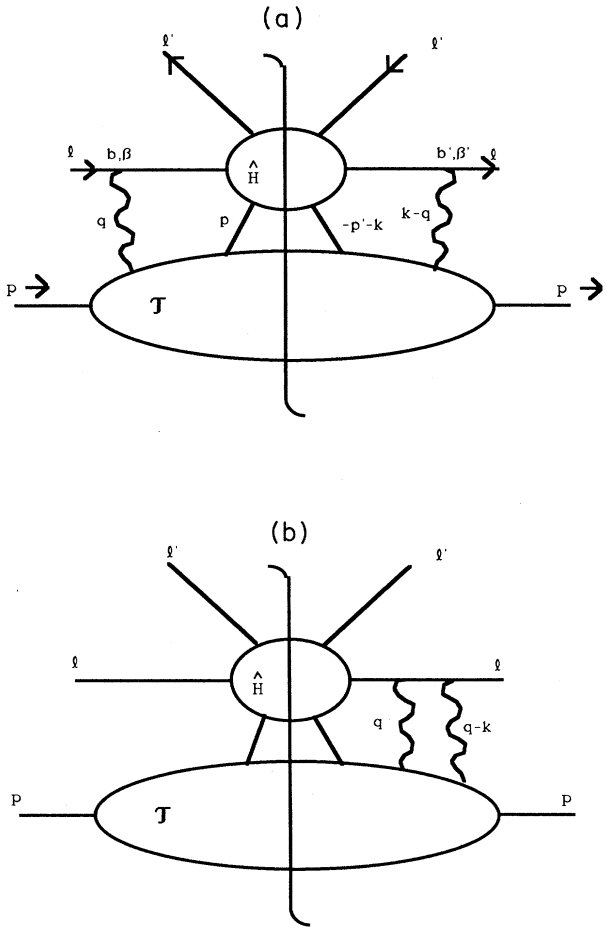

FIG. 2. Initial-state double scattering. $\hat{H}$ is the hard interaction. Momenta of vertical lines all flow up.

$$2w_{l'}\frac{d\sigma^{(i)}_{\rm soft}}{d^3l'}=(1+\delta_{i4})\frac{1}{2A\bar{s}}\int_{\Sigma_i}\frac{d^4q}{(2\pi)^4}\frac{d^4p'}{(2\pi)^4}\frac{dk^-}{2\pi}\times\sum_m \mathcal{P}^{(ia)\beta\beta'}_{m,bb'}\mathcal{T}^{bb'}_{m,\beta\beta'}$$

$$+\frac{1}{A\bar{s}}\mathrm{Re}\int_{\Sigma_i}\frac{d^4q}{(2\pi)^4}\frac{d^4p'}{(2\pi)^4}\frac{dk^-}{2\pi}\times\sum_m \mathcal{P}^{(ib)\beta\beta'}_{m,bb'}\tilde{\mathcal{T}}^{bb'}_{m,\beta\beta'}\ . \quad (4.2)$$

Here, β,β' (b,b') label the vector (color) indices of the exchanged soft gluons, and m labels the identity of the target parton of momentum p'^{μ}. $\bar{s}^{1/2}$ is the invariant mass of the projectile and an average nucleon in the target. $\mathcal{P}^{(j)}$ labels the projectile tensor of graph j, including the explicit propagators and vertices of the figure, as well as the hard subdiagram $\hat{H}_m$. $\mathcal{T}_m$ and $\tilde{\mathcal{T}}_m$ label the target tensors—the remainder of the graph, which includes the soft gluon propagators and the k^+ and $k_\perp$ integrals. Note the factor $(1+\delta_{i4})$, which takes into account the mirror diagram of Fig. 4(a). Only k^- dependence is kept in the $\mathcal{P}$'s, by the following reasoning.

In accordance with our comments above, we assume that the target tensors are nonvanishing only in a region in which $|k^{\mu}|<O(A^{-1/3})$ for all μ in its rest frame. Thus we assume that, to leading power in A, we may drop k^{μ} in the projectile tensors, unless $\mathcal{P}$ is a rapidly varying function of k^{μ}. This is only the case for k^- (in the target rest frame), since it is multiplied by $l^+=O(s)$.

Note that $\mathcal{T}_m$ is the same for all double-scattering graphs, and $\tilde{\mathcal{T}}_m$ for all absorption graphs. In the next section we analyze these tensors.

V. TARGET TENSORS

After a summation over final states, the double-scattering and interference diagram tensors may be written explicitly as

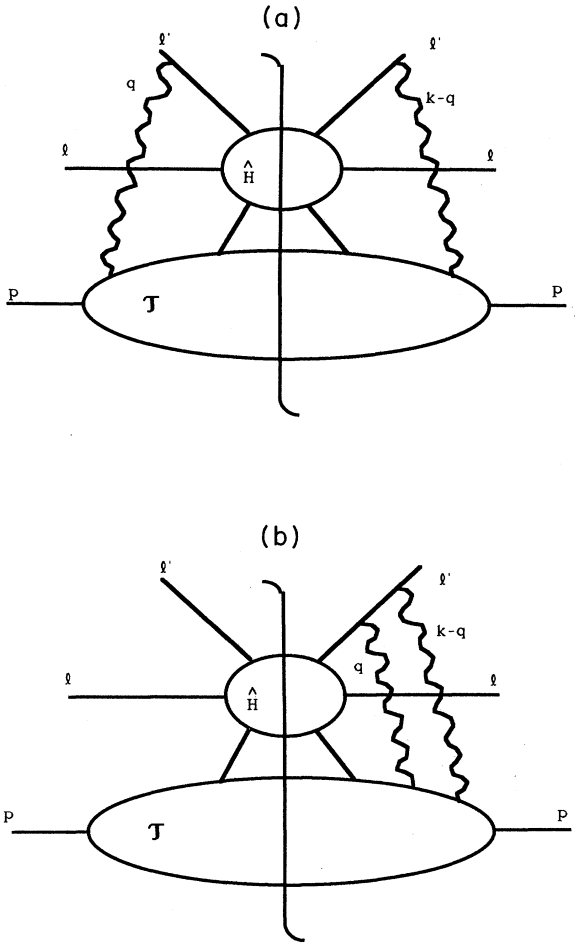

FIG. 3. Final-state double scattering.

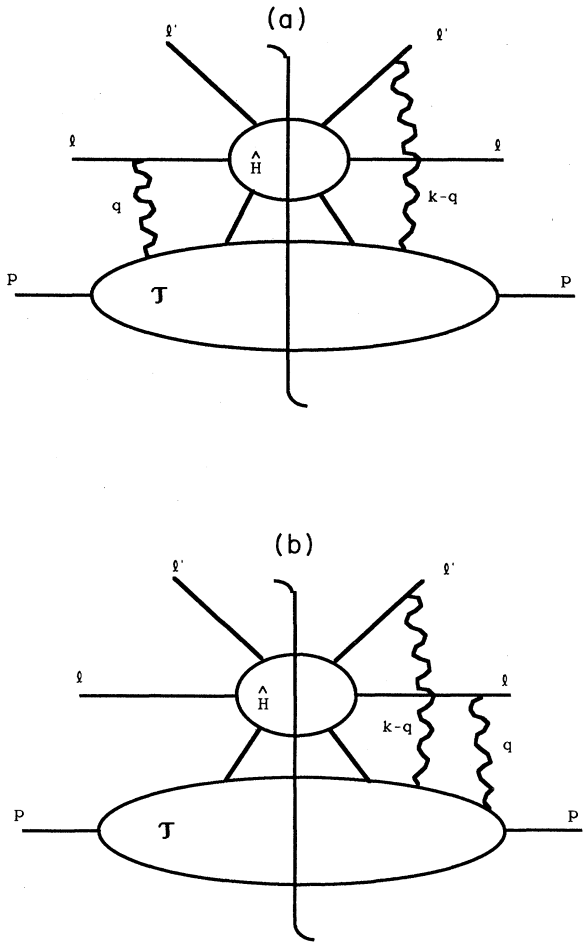

FIG. 4. Mixed initial- and final-state double scattering.

$$\mathcal{T}^{bb'}_{m,\beta\beta'} = \int d\eta\, d^4\xi_1 d^4\xi_2 \exp[-iq\cdot\xi_2 + ik^-u\cdot(\eta v+\xi_2/2) - ip'\cdot\xi_1]$$
$$\times\langle P|\bar{T}[\phi_m(\xi_1)A^{b'}_{\beta'}((\eta+\tfrac{1}{2}\xi_2\cdot u)v+\xi_1)]T[A^b_\beta((\eta+\tfrac{1}{2}\xi_2\cdot u)v-\xi_2+\xi_1)\phi_m(0)]|P\rangle\ , \tag{5.1}$$

$$\tilde{\mathcal{T}}^{bb'}_{m,\beta\beta'} = \int d\eta\, d^4\xi_1 d^4\xi_2 \exp[-iq\cdot\xi_2 + ik^-u\cdot(\eta v+\xi_2/2) - ip'\cdot\xi_1]$$
$$\times\langle P|\bar{T}[\phi^\dagger_m(\xi_1)A^{b'}_{\beta'}((\eta+\tfrac{1}{2}\xi_2\cdot u)v+\xi_1)A^b_\beta((\eta+\tfrac{1}{2}\xi_2\cdot u)v-\xi_2+\xi_1)]\phi_m(0)|P\rangle\ . \tag{5.2}$$

Here we have chosen the separation between the two ϕ fields as ξ_1^μ and between the two gauge fields as ξ_2^μ, and $v^\mu=\delta^{\mu^+}$ and $u^\mu=\delta^{\mu^-}$ are lightlike vectors in and opposite the projectile direction, respectively. The variable η thus roughly measures the separation between the two pairs of operators. This separation is lightlike because the k^+ and $\mathbf{k}_\perp$ integrals yield δ functions. To be more exact, k^+ and $\mathbf{k}_\perp$ should be cut off at $O(s/m)$ and $O(\sqrt{s}\,)$, respectively, since they are neglected in $\mathcal{P}$. Compared to the nuclear scale $(A^{1/3}R_0)^{-1}$, however, their ranges are essentially unbounded.

It may be worth noting that the matrix elements in (5.1) and (5.2) are related to the twist-four parton distributions of Refs. 11 and 12, at least in the limit where ξ_1^2 and ξ_2^2 vanish. This region might be expected to dominate when both q^2 and Q^2 are large, and the two scatterings are relatively well localized along the light cone.

To simplify (5.1) and (5.2), we treat the nucleus as a collection of A nucleons moving nonrelativistically in the nucleus rest frame. Thus, we decompose the nuclear state $\langle P|$ in terms of A-nucleon states $|p_1,p_2,\ldots,p_A\rangle$. Defining $d\tilde{p}\equiv d^3p/(2\pi)^3 2\omega_p$, we have, for instance,

$$\langle P|\bar{T}[\phi^\dagger_m(\xi_1)A^{b'}_{\beta'}((\eta+\tfrac{1}{2}\xi_2\cdot u)v+\xi_1)]T[A^b_\beta((\eta+\tfrac{1}{2}\xi_2\cdot u)v-\xi_2+\xi_1)\phi_m(0)]|P\rangle$$
$$=\int d\tilde{p}_1\cdots d\tilde{p}_A d\tilde{p}\,'_1\cdots d\tilde{p}\,'_A\langle P|p'_1,\ldots,p'_A\rangle\langle p'_1,\ldots,p'_A|\bar{T}[\phi^\dagger_m(\xi_1)A^{b'}_{\beta'}((\eta+\tfrac{1}{2}\xi_2\cdot u)v+\xi_1)]$$
$$\times T[A^b_\beta((\eta+\tfrac{1}{2}\xi_2\cdot u)v-\xi_2+\xi_1)\phi_m(0)]|p_1,\ldots,p_A\rangle$$
$$\times\langle p_1,\ldots,p_A|P\rangle\ . \tag{5.3}$$

We assume that nuclear interaction effects are small and that the nucleons carry essentially all of the momentum of the nucleus. This allows us to write the wave function as

$$\langle p_1,p_2\cdots p_A|P\rangle=[(2\pi)^3 2\omega_P]^{1/2}\delta^3\left[P-\sum_{i=1}^A p_i\right]\Psi_P(\{p_i\})\ , \tag{5.4}$$

where Ψ_P is a function appropriately symmetrized in the set $\{p_i\}$, whose normalization is set by requiring

$$\langle P'|P\rangle\equiv\int d\tilde{p}_1\cdots d\tilde{p}_A\langle P'|p_1,\ldots,p_A\rangle\langle p_1,\ldots,p_A|P\rangle=(2\pi)^3 2\omega_P\delta^3(P'-P)\ . \tag{5.5}$$

Substituting (5.4) into (5.3) and assuming that the operator in (5.3) acts on pairs of nucleons, we obtain

$$\langle P|\bar{T}[\phi^\dagger_m(\xi_1)A^{b'}_{\beta'}((\eta+\tfrac{1}{2}\xi_2\cdot u)v+\xi_1)]T[A^b_\beta((\eta+\tfrac{1}{2}\xi_2\cdot u)v-\xi_2+\xi_1)\phi_m(0)]|P\rangle$$
$$=(2\pi)^3 2\omega_P\int d\tilde{p}\,'_1 d\tilde{p}\,'_2 d\tilde{p}_1 d\tilde{p}_2\delta^3(p_1+p_2-p'_1-p'_2)\langle p'_1,p'_2|\bar{T}[\phi^\dagger_m(\xi_1)A^{b'}_{\beta'}((\eta+\tfrac{1}{2}\xi_2\cdot u)v+\xi_1)]$$
$$\times T[A^b_\beta((\eta+\tfrac{1}{2}\xi_2\cdot u)v-\xi_2+\xi_1)\phi_m(0)]|p_1,p_2\rangle$$
$$\times\langle p'_1,p'_2|d_2|p_1,p_2\rangle\ , \tag{5.6}$$

where

$$\langle p'_1,p'_2|d_2|p_1,p_2\rangle\equiv\int\left[\prod_{i=3}^A d\tilde{p}_i\right]\delta^3\left[P-\sum_{i=1}^A p_i\right]\Psi^*_P(p'_1,p'_2,p_3,\ldots,p_A)\Psi_P(p_1,p_2,p_3,\ldots,p_A) \tag{5.7}$$

is a two-particle density matrix. We discuss the field matrix element and density matrix in turn.

The field matrix element in Eq. (5.6) may be further simplified by assuming that the constituent nucleons scatter independently. Different contractions correspond to different physical processes. For instance, the contraction

$$\langle p'_1|\bar{T}[\phi^\dagger_m(\xi_1)A^{b'}_{\beta'}((\eta+\tfrac{1}{2}\xi_2\cdot u)v+\xi_1)]|p_1\rangle\langle p'_2|T[A^b_\beta((\eta+\tfrac{1}{2}\xi_2\cdot u)v-\xi_2+\xi_1)\phi_m(0)]|p_2\rangle \tag{5.8}$$

describes double elastic scattering of individual nucleons, and is highly suppressed compared to the dominant inelastic process. Also, we expect that the density matrix, Eq. (5.7), vanishes for $|\mathbf{p}_i-\mathbf{p}'_i|\gg(A^{1/3}R_0)^{-1}$. Then the fact that $Q_\perp$ is large leads to the suppression of the contraction

$$\langle p'_1|\phi^\dagger_m(\xi_1)A^b_\beta((\eta+\tfrac{1}{2}\xi_2\cdot u)v-\xi_2+\xi_1)|p_1\rangle\langle p'_2|A^{b'}_{\beta'}((\eta+\tfrac{1}{2}\xi_2\cdot u)v+\xi_1)\phi_m(0)|p_2\rangle\ . \tag{5.9}$$

This leaves only contractions which pair the two ϕ fields and the two A fields. So, we make the replacement

$$\langle p_1',p_2'|\bar{T}[\phi_m^\dagger(\xi_1)A_{\beta'}^{b'}((\eta+\tfrac{1}{2}\xi_2\cdot u)v+\xi_1)]T[A_\beta^b((\eta+\tfrac{1}{2}\xi_2\cdot u)v-\xi_2+\xi_1)\phi_m(0)]|p_1,p_2\rangle$$
$$\to\frac{\delta_{bb'}}{8}\langle p_1'|\phi_m^\dagger(\xi_1)\phi_m(0)|p_1\rangle\langle p_2'|A_{\beta'}^{b'}((\eta+\tfrac{1}{2}\xi_2\cdot u)v+\xi_1)A_\beta^b((\eta+\tfrac{1}{2}\xi_2\cdot u)v-\xi_2+\xi_1)|p_2\rangle\ , \tag{5.10}$$

where we have used the color-singlet nature of the nucleon.

Now let us treat the density matrix. The assumption that we may ignore two-particle correlations to leading power in A allows us to write

$$\langle \mathbf{p}_1',\mathbf{p}_2'|d_2|\mathbf{p}_1,\mathbf{p}_2\rangle=\langle \mathbf{p}_1'|d_1|\mathbf{p}_1\rangle\langle \mathbf{p}_2'|d_1|\mathbf{p}_2\rangle\ . \tag{5.11}$$

Here $\langle \mathbf{p}'|d_1|\mathbf{p}\rangle$ is a one-particle momentum density matrix, which may be written in terms of a configuration-space density matrix as

$$\langle \mathbf{p}'|d_1|\mathbf{p}\rangle=\sqrt{4\omega_p\omega_{p'}}\int d^3R\,d^3r\langle \mathbf{x}'|d_1|\mathbf{x}\rangle \times e^{-i\mathbf{R}\cdot(\mathbf{p}'-\mathbf{p})-i\mathbf{r}\cdot 1/2(\mathbf{p}'+\mathbf{p})}\ , \tag{5.12}$$

where

$$\mathbf{R}=\tfrac{1}{2}(\mathbf{x}'+\mathbf{x}),\quad \mathbf{r}=\mathbf{x}'-\mathbf{x}\ . \tag{5.13}$$

By construction, the diagonal matrix elements of d_1 give the particle density, which we represent as

$$\langle \mathbf{x}|d_1|\mathbf{x}\rangle=\frac{9}{16\pi^2R_0^6}\rho(\mathbf{x})\ , \tag{5.14}$$

with R_0 the average internucleon separation. We assume that d_1 decreases for $\mathbf{x}'\neq\mathbf{x}$, and that this decrease is described by a rotation and translation invariant function $r(|\mathbf{x}'-\mathbf{x}'|)$, normalized by $r(0)=1$, except near the nuclear surface. We assume $r(x)$ decreases on a scale small compared to $R_0A^{1/3}$. Then, up to surface corrections, which we expect to be suppressed by $O(A^{-1/3})$, we have

$$\langle \mathbf{x}'|d_2|\mathbf{x}\rangle=\frac{9}{16\pi^2R_0^6}\rho\left[\frac{\mathbf{x}+\mathbf{x}'}{2}\right]r(|\mathbf{x}-\mathbf{x}'|)\ . \tag{5.15}$$

For a homogeneous spherical nucleus centered at the origin, this is

$$\langle \mathbf{x}'|d_2|\mathbf{x}\rangle=\frac{9}{16\pi^2R_0^6}\theta\left[R-\left|\frac{\mathbf{x}+\mathbf{x}'}{2}\right|\right]r(|\mathbf{x}-\mathbf{x}'|)\ . \tag{5.16}$$

More complex and realistic forms for the density matrix are, of course, possible. Using (5.15) in (5.12) gives

$$\langle \mathbf{p}'|\rho_1|\mathbf{p}\rangle=\sqrt{4\omega_p\omega_{p'}}\frac{9}{16\pi^2R_0^6}\tilde{\rho}(\Delta\mathbf{p})\tilde{r}(\mathbf{P})\ , \tag{5.17}$$

where $\tilde{\rho}$ and $\tilde{r}$ are the Fourier transforms of ρ and r, respectively, and where

$$\mathbf{P}=\tfrac{1}{2}(\mathbf{p}+\mathbf{p}'),\quad \Delta\mathbf{p}=\mathbf{p}'-\mathbf{p} \tag{5.18}$$

are conjugate to $\mathbf{r}$ and $\mathbf{R}$, respectively. For fixed $|\Delta\mathbf{p}|$, we expect $\tilde{\rho}(\Delta\mathbf{p})$ to decrease with A, and we shall assume that this decrease is fast compared to the variations in $\Delta\mathbf{p}$ of nucleon matrix elements of the form $\langle \mathbf{p}'|(\text{fields})|\mathbf{p}\rangle$, since these matrix elements are determined by nucleon, rather than nuclear, scales. In contrast, $\tilde{r}(\mathbf{P})$ need not decrease with A, since $r(x)$ is a universal function. So, $\tilde{r}(\mathbf{P})$ may be taken to describe the (Fermi) momentum distribution of nucleons in the nucleus.

We are now ready to give an explicit form for the target tensor (5.1) by using Eqs. (5.10), (5.11), and (5.17) in the matrix element (5.6). This gives

$$\begin{aligned}\mathcal{T}_{m,\beta\beta'}^{bb'}=2\omega_P\int d^4\xi_1d^4\xi_2e^{-ip'\cdot\xi_1-iq\cdot\xi_2}&\\ \times\int d\eta e^{ik^-u\cdot(\eta v+\xi_2/2)}\int d^3y\int d^3\tilde{p}_1d^3\tilde{p}\,'_1e^{+i\Delta\mathbf{p}_1\cdot(\mathbf{y}+1/2\xi_1)}(4\omega_{p_1}\omega_{p_1'})^{1/2}&\left[\frac{9}{16\pi^2R_0^6}\right]\tilde{\rho}(\Delta\mathbf{p}_1)\\ \times\tilde{r}(\mathbf{P}_1)\langle p_1'|\phi_m^\dagger(\tfrac{1}{2}\xi_1)\phi_m(-\tfrac{1}{2}\xi_1)|p_1\rangle&\\ \times\frac{\delta_{bb'}}{8}\int d^3\tilde{p}_2d^3\tilde{p}\,'_2e^{+i\Delta\mathbf{p}_2\cdot\mathbf{y}}(4\omega_{p_2}\omega_{p_2'})^{1/2}&\left[\frac{9}{16\pi^2R_0^6}\right]\tilde{\rho}(\Delta\mathbf{p}_2)\\ \times e^{+i\Delta\mathbf{p}_2\cdot(\eta v+\xi_1-\hat{\xi}_2/2)}&\\ \times\tilde{r}(\mathbf{P}_2)\left\langle p_2'\left|A_{\beta'}^d\left[\frac{\xi_2}{2}\right]A_\beta^d\left[-\frac{\xi_2}{2}\right]\right|p_2\right\rangle\ ,&\end{aligned} \tag{5.19}$$

where $\hat{\xi}_2^\mu=\xi_2^\mu-(\xi_2\cdot u)v^\mu=(0^+,\xi_2^-,\xi_{2\perp})$, and where we have represented the factor $(2\pi)^3\delta^3(\mathbf{p}_1+\mathbf{p}_2-\mathbf{p}_1'-\mathbf{p}_2')$ in Eq. (5.6) as an integral over the variable $\mathbf{y}$. We now make a crucial further approximation. Consider the $\mathbf{p}_2$ and $\mathbf{p}_2'$ integrals, which can be carried out in terms of $\mathbf{P}_2=\frac{1}{2}(\mathbf{p}_2+\mathbf{p}_2')$ and $\Delta\mathbf{p}_2=\mathbf{p}_2-\mathbf{p}_2'$. As we observed above, we expect the function

$\tilde{\rho}(\Delta\mathbf{p}_2)$ to be more sharply peaked in $|\Delta\mathbf{p}_2|$ than $\tilde{r}(\mathbf{P}_2)$ is in $|\mathbf{P}_2|$ and than the nucleon matrix element $\langle p_2'|A_{\beta'}^{d}(\xi_2/2)A_{\beta}^{d}(-\xi_2/2)|p_2\rangle$ is in $\Delta\mathbf{p}_2$. As a matter of fact, this last point is a subtle one. For, inserting a complete set of states in the two-field matrix element gives

$$\langle p_2'|A_{\beta'}^{d}((\eta+\tfrac{1}{2}\xi_2\cdot u)v+\xi_1)A_{\beta}^{d}((\eta+\tfrac{1}{2}\xi_2\cdot u)v-\xi_2+\xi_1)|p_2\rangle$$

$$=\exp[i\Delta\mathbf{p}_2\cdot(\eta\mathbf{v}+\boldsymbol{\eta}_1-\hat{\boldsymbol{\xi}}_2)]\sum_n \exp[i(p_2+p_2'-2p_n)\cdot\xi_2/2]\langle p_2'|A_{\beta'}^{d}(0)|p_n\rangle\langle p_n|A_{\beta}^{d}(0)|p_2\rangle\ , \quad (5.20)$$

where the vector $\mathbf{v}$ is the spatial part of the vector v^μ in the projectile direction. We have also explicitly removed the phase in the second matrix associated with the vector $\eta v^\mu+\xi_1^\mu$, assuming that Δp^0 is a small number compared to $\Delta\mathbf{p}$, as is appropriate for nonrelativistic motion of the constituents. Because $\tilde{\rho}(\Delta\mathbf{p}_2)$ is sharply peaked about $\Delta\mathbf{p}_2=0$ as $A\to\infty$, we may reasonably set $\Delta\mathbf{p}_2$ to zero in the matrix element, which then becomes diagonal for the purposes of the $\Delta\mathbf{p}_2$ integration in (5.19). This step is justified, however, only after the explicit phase $e^{i\Delta\mathbf{p}_2\cdot(\mathbf{v}\eta+\xi_1-\hat{\xi}_2)}$ is factored from the matrix element by translation invariance, since the scale of the vector $\eta\mathbf{v}+\xi_1-\hat{\xi}_2$ is as yet undetermined. In the remaining matrix element

$$\langle p_2'|A_{\beta'}^{d}(\xi_2/2)A_{\beta}^{d}(-\xi_2/2)|p_2\rangle\ ,$$

the $\Delta\mathbf{p}_2$ dependence is entirely in factors such as $\langle p_2-\frac{1}{2}\Delta p_2|A_{\beta'}^{d}(0)|p_n\rangle$, which depends only on nucleonic scales. By similar reasoning, we set $\Delta\mathbf{p}$ to zero in the factors $4\omega_{p_i}\omega_{p_i'}$ which become $4\omega_{P_i}^2$ in Eq. (5.19).

Once $\Delta\mathbf{p}_2$ is set to zero in the matrix element, as well as the flux factor, the remaining $\Delta\mathbf{p}_2$ integral gives the reverse Fourier transform of $\tilde{\rho}(\Delta p_2)$, that is, $\rho(\mathbf{y}+\eta\mathbf{v}+\xi_1-\hat{\xi}_2)$. Going through the same procedure for the $\mathbf{p}_1,\mathbf{p}_1$ integral will give $\rho(\mathbf{y}-\xi_1/2)$ times the diagonal matrix element

$$\langle P_1|\phi_m^\dagger(\xi_1/2)\phi_m(-\xi_1/2)|P_1\rangle\ .$$

Before giving the final result, we observe that in the region of interest the parton with momentum p'^μ in Fig. 2 is energetic (large x). We thus expect the Fourier transform of the p_1 matrix element to be dominated by—if not short distances in the target rest frame—at least distances which do not grow with A. Hence, we claim that, up to surface corrections, we may neglect ξ_1 compared to $\mathbf{y}$ in Eq. (5.19). In addition, as we shall see below, $\mathbf{q}_T$ and q^+ are not fixed to be small. So, we expect the p_2 matrix elements to be suppressed once $\hat{\xi}_2^\mu$ reaches nucleon scales. Hence, we also neglect $\Delta\mathbf{p}_2\cdot\hat{\xi}_2$ below. With this in mind, we may now write Eq. (5.19) to leading order in A as

$$\mathcal{T}_{m,\beta'\beta}^{b'b}=2\omega_P\left[\frac{9}{16\pi^2R_0^6}\right]^2$$
$$\times\int d^3y\int d\eta\, e^{ik^-\eta}\rho(\mathbf{y})\rho(\mathbf{y}+\eta\mathbf{v})\int d^4\xi_1 e^{-ip'\cdot\xi_1}\int d^3\tilde{P}_1\tilde{r}(P_1)\langle P_1|\phi_m^\dagger(\xi_1/2)\phi_m(-\xi_1/2)|P_1\rangle$$
$$\times\frac{\delta_{bb'}}{8}\int d^4\xi_2 e^{-i(q-1/2k^-u)\cdot\xi_2}$$
$$\times\int d^3\tilde{P}_2\tilde{r}(P_2)\langle P_2|A_{\beta'}^{d}(\xi_2/2)A_{\beta}^{d}(-\xi_2/2)|P_2\rangle\ , \quad (5.21)$$

where $d^3\tilde{P}_i\equiv d^3\mathbf{P}_i/2\omega_{P_i}$. In this form, the target matrix is a geometrical factor times the Fourier transforms of two constituent nucleon matrix elements, each averaged over the constituent's momentum. This is the form of $\mathcal{T}$ which we will use below. Almost identical reasoning may be applied to $\bar{\mathcal{T}}$ which appears in Figs. 2(b), 3(b), and 4(b), with the result

$$\bar{\mathcal{T}}_{m,\beta'\beta}^{b'b}=2\omega_P\left[\frac{9}{16\pi^2R_0^6}\right]^2$$
$$\times\int d^3y\, d\eta\, e^{ik^-\eta}\rho(\mathbf{y})\rho(\mathbf{y}+\eta\mathbf{v})\int d^4\xi_1 e^{-ip'\cdot\xi_1}\int d^3\tilde{P}_1\tilde{r}(P_1)\langle P_1|\phi_m^\dagger(\xi_1/2)\phi_m(-\xi_1/2)|P_1\rangle$$
$$\times\frac{\delta_{bb'}}{8}\int d^4\xi_2 e^{-i(q-1/2k^-u)\cdot\xi_2}$$
$$\times\int d^3\tilde{P}_2\tilde{r}(P_2)\langle P_2|\bar{T}(A_{\beta'}^{d}(\xi_2/2)A_{\beta}^{d}(-\xi_2/2))|P_2\rangle\ . \quad (5.22)$$

The only difference from (5.21) is in the second matrix element, which involves the anti-time-ordered product.

VI. PROJECTILE TENSORS AND FACTORIZATION

We now analyze the projectile tensors $\mathcal{P}^{(j)}$ in Eq. (4.2). For definiteness, we choose the initial-state double-scattering diagram, Fig. 2(a), to illustrate the method. We take the incident and final partons to be quarks; essentially identical reasoning can be given for antiquarks and gluons. $\mathcal{P}^{2(a)}$ is given by

$$\mathcal{P}^{2(a)\beta'\beta}_{m,b'b}=g^2\tfrac{1}{6}\mathrm{tr}[\not{l}\gamma^{\beta'}T_{b'}(\not{l}+\not{q}-\hat{\not{k}})^{-1}\times\hat{H}^{2(a)}_m(l^\mu,Q^\mu,p'^\mu,q^\mu,k^-)\times(\not{l}+\not{q})^{-1}\gamma^\beta T_b]\ , \tag{6.1}$$

$$\hat{H}^{2(a)}_m=K^{*2(a)}_m\not{l}'H^{2(a)}_m\ . \tag{6.2}$$

The factor $\frac{1}{6}$ is for the spin and color average of the incoming projectile quark. In accordance with the discussion of Sec. IV, $\hat{k}^\mu=k^\mu\delta^{\mu^-}$ and we have dropped $\mathbf{k}_\perp$ and k^+ dependence in $\mathcal{P}$.

We have described Fig. 2(a) as an initial-state interaction, and this suggests that we do momentum integrals in a way that makes this time-ordering manifest. This can be accomplished by performing the q^- and k^- integrals first, using the explicit exponentials in the target tensor, Eq. (5.21). These integrals can be done by closing the q^- and k^- contours in the upper or lower half-plane, depending on the sign of the coefficient of q^- and k^- in the exponentials. The integral then equals the sum of the residues of propagator poles (if any) enclosed, times θ functions involving η and ξ_2^+. In general, k^- and q^- appear in propagators internal to $\hat{H}^{2(a)}_m$, as well as in the explicit quark propagators in Eq. (6.1). Putting the former on-shell, however, requires q^- and/or k^- to be large, typically of order $Q_\perp^2/Q^+$. This forces the explicit quark propagators far off-shell, and large q^- or k^- are not associated with enhancements in A. We therefore ignore poles in $\hat{H}^{2(a)}_m$ for the purposes of the q^- and k^- integrations. Using (5.21), these integrals become

$$Q^{2(a)\beta'\beta}_{m,b'b}=\int_{-\infty}^{\infty}\frac{dq^-dk^-}{(2\pi)^2}e^{-i(q^--k^-/2)\xi_2^++ik^-\eta}\mathcal{P}^{2(a)\beta'\beta}_{mb'b}\ . \tag{6.3}$$

The k^- and q^- integrals are easily carried out by the method described above, and

$$Q^{2(a)\beta'\beta}_{m,b'b}=g^2\theta(\xi_2^+/2-\eta)\theta(-\xi_2^+/2-\eta)[4(l^++q^+)]^{-2}\times\exp[-iq_\perp^2\xi_2^+/2(l^++q^+)]\times\tfrac{1}{6}\mathrm{tr}[\not{l}\gamma^{\beta'}T_{b'}(\not{l}-\not{q})\hat{H}^{2(a)}_m(\not{l}+\not{q})\gamma^\beta T_b]\ . \tag{6.4}$$

In Fig. 2(a) $k^-=0$. Because $Q^{2(a)}$ is multiplied by $\mathcal{T}$, Eq. (5.21), which is proportional to $\delta_{bb'}$, the color matrices $T_bT_{b'}$ may be replaced by $\frac{1}{8}\delta_{bb'}C_F$. The Dirac trace may be reduced, using helicity conservation (we work, of course, with massless quarks), to

$$t^{\beta'\beta}=\sum_h\mathrm{tr}\{\not{l}\gamma^{\beta'}(\not{l}+\not{q})\tfrac{1}{2}[1-(-1)^h\gamma_5]\gamma^\beta\}\times\bar{u}_h(l+q)\hat{H}^{2(a)}_m u_h(l+q)\ , \tag{6.5}$$

where $h=\pm1$ is the helicity of the incoming quark. If the target is unpolarized, the γ_5 term in Eq. (6.5) does not survive in Eq. (4.2), because the target tensor is symmetric. That is,

$$t^{\beta'\beta}=\left[4l^\beta l^{\beta'}+2l^{\beta'}q^\beta+2q^{\beta'}l^\beta+g^{\beta\beta'}\frac{q^2}{2}\right]\times\sum_h\bar{u}_h(l+q)\hat{H}^{2(a)}_m u_h(l+q)+A^{\beta\beta'}\ , \tag{6.6}$$

where $A^{\beta\beta'}$ does not contribute to Eq. (4.2). We now use Ward identities to show that only the first term in parenthesis in Eq. (6.6) contributes to our final answer.

For this purpose, we note that the leading term in Eq. (6.6) is proportional to $4l^\beta l^{\beta'}=4(l^+)^2v^\beta v^{\beta'}$. The fourth term is thus suppressed by $q^2/(l^+)^2=O(q^2m^2/s^2)$. A suppression by two powers of s in the soft region is sufficient to neglect this term. The second and third terms are suppressed by a single power of s only. They are, however, proportional to q^β, so that in their contributions to Eq. (4.2), one of the gluon fields, either A^d_β or $A^d_{\beta'}$ in Eq. (5.21), is contracted into a longitudinal polarization. Inserting a complete set of states between the gluon fields, both contributions are proportional to matrix elements such as

$$q^\beta\langle p_i|A^d_\beta(0)|n\rangle=0\ , \tag{6.7}$$

where $|n\rangle$ is a physical intermediate state. This gives, in Eq. (6.4),

$$Q^{2(a)\beta'\beta}_{m,b'b}=g^2C_F\theta(\xi_2^+/2-\eta)\theta(-\xi_2^+/2-\eta)\times\frac{\delta_{b'b}}{8}v^{\beta'}v^\beta\left[\frac{l^+}{l^++q^+}\right]^2\times\exp[-iq_\perp^2\xi_2^+/2(l^++q^+)]\times\tfrac{1}{6}\mathrm{tr}[(\not{l}+\not{q})K^{2(a)*}_m\not{l}'H^{2(a)}_m]\ , \tag{6.8}$$

where we have used (6.2) for the hard part to exhibit the fermion spin structure. We should note, however, that the functions $H^{2(a)}$ and $K^{2(a)}$ have implicit indices for parton m.

We can define a similar quantity for each of the remaining diagrams in Figs. 2–4. The initial-state interference graph, Fig. 2(b), and the double-scattering and interference graphs, Figs. 3(a) and 3(b) may be treated in an almost identical manner to Fig. 2(a). The results are

$$Q^{2(b)\beta'\beta}_{m,b',b}=-g^2C_F\theta(-\xi_2^+)\theta(-\eta+\xi_2^+/2)\frac{\delta_{b'b}}{8}v^{\beta'}v^{\beta}\left[\frac{l^+}{l^++q^+}\right]\exp[-iq_\perp^2\xi_2^+/2(l^++q^+)]\tfrac{1}{6}\mathrm{tr}(\not{l}K_m^{*2(b)}\not{l}'H_m^{2(b)}) , \quad (6.9)$$

$$Q^{3(a)\beta'\beta}_{m,b'b}=g^2C_F\theta(\eta^++\xi_2^+/2)\theta(\eta^+-\xi_2^+/2)\frac{\delta_{b'b}}{8}v'^{\beta'}v'^{\beta}\left[\frac{u'\cdot l'}{l'^+-q^+}\right]^2\exp\left[i\frac{-2\mathbf{Q}_\perp\cdot\mathbf{q}_\perp+\mathbf{q}_\perp^2+2l'^-q^+}{2(l'^+-q^+)}\xi_2^+\right]$$

$$\times\tfrac{1}{6}\mathrm{tr}[\not{l}K_m^{*3(a)}(\not{l}'-\not{q})H_m^{3(a)}] , \quad (6.10)$$

$$Q^{3(b)\beta'\beta}_{m,b'b}=-g^2C_F\theta(\eta^+-\tfrac{1}{2}\xi_2^+)\theta(-\xi_2^+)\frac{\delta_{b'b}}{8}v'^{\beta'}v'^{\beta}\left[\frac{(u'\cdot l')^2}{(l'^+-q^+)l'^+}\right]\exp\left[i\frac{-2\mathbf{Q}_\perp\cdot\mathbf{q}_\perp+\mathbf{q}_\perp^2+2l'^-q^+}{2(l'^+-q^+)}\xi_2^+\right]$$

$$\times\tfrac{1}{6}\mathrm{tr}(\not{l}K_m^{*3(b)}\not{l}'H_m^{3(b)}) . \quad (6.11)$$

Here we define the lightlike vectors v'^{β} and u'^{β} by the requirements

$$l'^{\beta}=(u'\cdot l')v'^{\beta}, \quad u'\cdot v'=1 . \quad (6.12)$$

That is, v'^{β} is a lightlike vector in the $\mathbf{l}'$ direction, while

$$u'^{\beta}=(v'^0,-\mathbf{v}')\frac{1}{\sqrt{v'^2+\mathbf{v}'^2}} . \quad (6.13)$$

The mixed-state diagrams, Figs. 4(a) and 4(b), also give similar results, although their evaluation involves a few slight differences. First, we find that k^- no longer vanishes for $k^+=|\mathbf{k}_\perp|=0$; rather, we have

$$q^-=\frac{\pm\mathbf{q}_\perp^2}{2(l^+\pm q^+)}, \quad k^-=\frac{\pm\mathbf{q}_\perp^2}{2(l^+\pm q^+)}+\frac{2l'^-q^+-2\mathbf{Q}_\perp\cdot\mathbf{q}_\perp+\mathbf{q}_\perp^2}{2(l'^+-q^+)} . \quad (6.14)$$

Second, we cannot reduce the trace in quite the same manner as in Eq. (6.5). To see this, we apply helicity conservation to the Dirac trace in Fig. 4(a),

$$T^{4(a)\beta'\beta}=\{\not{l}K_m^{*4(a)}(\not{l}'+\hat{\not{k}}-\not{q})\gamma^{\beta'}T_{b'}\not{l}'H_m^{4(a)}(\not{l}+\not{q})\gamma^{\beta}T_b\}$$

$$=\sum_{hh'}\bar{u}_h(l)K_m^{*4(a)}T_{b'}u_{h'}(l'+\hat{k}-q)\bar{u}_{h'}(l')H_m^{4(a)}T_bu_h(l+q)\bar{u}_h(l+q)\gamma^{\beta}u_h(l)\bar{u}_{h'}(l'+\hat{k}-q)\gamma^{\beta'}u_{h'}(l') , \quad (6.15)$$

where the color trace is understood. Here, unlike in Eq. (6.5), the spinors no longer pair in the form of projection operators. We can, however, expand scalars of the form $\bar{u}_h(l+q)\gamma^{\beta}u_h(l)$ around $q^\mu=0$, by using the relation

$$u(l^+v^\mu+q^\mu)=\left[1+\frac{1}{4l^+}[\not{q},\gamma^-]\right]u(l^+v^\mu)+O((l^+)^{-2}) , \quad (6.16)$$

which follows from the fact that the matrix $\Lambda^\mu_\nu=\delta_{\nu^+}(q^\mu/l^+)+O((l^+)^{-2})$ transforms the vector $l^\mu=l^+\delta^{\mu+}$ into $l^\mu+q^\mu$. Using Eq. (6.16) in Eq. (6.15),

$$T^{4(a)\beta'\beta}=4l^{\beta}l'^{\beta'}\sum_h\bar{u}_h(l)K_m^{*4(a)}T_{b'}u(l'+\hat{k}-q)u_h(l')T_bH_m^{4(a)}u_h(l+q) . \quad (6.17)$$

Unlike Figs. 2 and 3, the trace in Figs. 4(a) and 4(b) is of the form of a cross section only for $q^\mu=0$. In any case, corresponding to Eqs. (6.8)–(6.11), we find

$$Q^{4(a)\beta'\beta}_{m,b'b}=g^2\theta(\xi_2^+/2+\eta)\theta(\xi_2^+/2-\eta)v'^{\beta'}v^{\beta}\left[\frac{l'^+(u'\cdot l')}{(l'^+-q^+)(l^++q^+)}\right]$$

$$\times\exp\left[-\frac{i\mathbf{q}_\perp^2\xi_2^+}{2(l^++q^+)}+i\left[\frac{\mathbf{q}_\perp^2}{2(l^++q^+)}+\frac{2l'^-q^+-2\mathbf{Q}_\perp\cdot\mathbf{q}_\perp+\mathbf{q}_\perp^2}{2(l'^+-q^+)}\right](\eta+\xi_2^+/2)\right]$$

$$\times\tfrac{1}{6}\sum_h\bar{u}_h(l)K_m^{*4(a)}T_{b'}u_h(l'+\hat{k}-q)\bar{u}_h(l')H_m^{4(a)}T_bu_h(l+q) \quad (6.18)$$

and

$$Q^{4(a)\beta'\beta}_{m,b'b}=-g^2\theta(\xi_2^+/2+\eta)\theta(\xi_2^+/2-\eta)v'^{\beta'}v^{\beta}\left[\frac{l^+(u\cdot l')}{(l'^+-q^+)(l^+-q^+)}\right]$$
$$\times\exp\left[\frac{+i\mathbf{q}_\perp^2\xi_2^+}{2(l^+-q^+)}+i\left[\frac{-\mathbf{q}_\perp^2}{2(l^+-q^2)}+\frac{2l'^-q^+-2\mathbf{Q}_\perp\cdot\mathbf{q}_\perp+\mathbf{q}_\perp^2}{2(l'^+-q^+)}\right](\eta+\xi_2^+/2)\right]$$
$$\times\tfrac{1}{6}\sum_h\bar{u}_h(l-q)K_m^{*4(b)}T_{b'}u_h(l'+\hat{k}-q)\bar{u}_h(l')H_m^{4(b)}T_bu_h(l)\ . \tag{6.19}$$

Finally, substituting Eqs. (5.20), (5.21), and the Q's in (4.2) we can write the following expression for the contribution of diagram i ($i=2,3,4$) to the soft double-scattering cross section:

$$2w_{l'}\frac{d\sigma^{(i)}_{\rm soft}}{d^3l'}=\int_{\Sigma_i}\frac{dq^+d^2\mathbf{q}_\perp}{(2\pi)^3}\int dk^-dq^-[(1+\delta_{i4})\mathcal{S}^{i(a)}(q,k^-,l)\sigma_{i(a)}(l,l',q,k^-)\delta(k^--k_{i(a)})\delta(q^--q_{i(a)})$$
$$+2\,\mathrm{Re}\mathcal{S}^{i(b)}(q,k^-,l)\sigma_{i(b)}(l,l',q,k^-)\delta(k^--k_{i(b)})\delta(q^--q_{i(b)})]\ . \tag{6.20}$$

Here, the double-scattering [i(a)] and interference [i(b)] terms each appear as an integral of the product of a "hard" factor σ and a "soft" factor $\mathcal{S}$. $k_{i(a),(b)}$ and $q_{i(a),(b)}$ are functions of $\mathbf{q}_T$ and q^+,

$$q_{2(a)}=q_{2(b)}=\mathbf{q}_\perp^2/2(l^++q^+),\quad k_{2(a)}=k_{2(b)}=0\ ,$$
$$q_{3(a)}=q_{3(b)}=-\frac{-2\mathbf{Q}_\perp\cdot\mathbf{q}_\perp+\mathbf{q}_\perp^2+2l'^-q^+}{2(l'^+-q^+)},\quad k_{3(a)}=k_{3(b)}=0\ ,$$
$$q_{4(a)}=\frac{\mathbf{q}_\perp^2}{2(l^++q^+)},\quad k_{4(a)}=q_{4(a)}+\frac{-2\mathbf{Q}_\perp\cdot\mathbf{q}_\perp+\mathbf{q}_\perp^2+2l'^-q^+}{2(l'^+-q^+)}\ , \tag{6.21}$$
$$q_{4(b)}=\frac{-\mathbf{q}_\perp^2}{2(l^+-q^+)},\quad k_{4(b)}=q_{4(b)}+\frac{-2\mathbf{Q}_\perp\cdot\mathbf{q}_\perp+\mathbf{q}_\perp^2+2l'^-q^+}{2(l'^+-q^+)}\ .$$

The soft factor for Fig. 2(a) is defined as

$$\mathcal{S}^{2(a)}=g^2(Q^2)\frac{l^+}{l^++q^+}\int d^4\xi_2\exp(-iq\cdot\xi_2)\int d^3\tilde{P}_2\bar{r}(\mathbf{P}_2)\langle P_2|v\cdot A^d(\xi_2/2)v\cdot A^d(-\xi_2/2)|P_2\rangle U(\xi_2^+/2\sqrt{2},R,0)\ . \tag{6.22}$$

The function U is a geometrical factor,

$$U(\chi,R,k^-)=\frac{9}{16\pi^2R_0^6}\int d^3y\,\rho(\mathbf{y})\int_{-\infty}^{-|\chi|}d\alpha\,e^{+i\sqrt{2}k^-\alpha}\rho(\mathbf{y}+\alpha\mathbf{n})\ , \tag{6.23}$$

where $\alpha=\eta/\sqrt{2}$ is the 3 component of the vector $\eta v^\mu=\eta\delta^{\mu+}$, and $\mathbf{n}$ is a unit vector in the 3 direction. The upper limit on the α integral is the effect of the θ functions linking η and ξ_2^+ in Eq. (6.8). For a spherical homogeneous nucleus, the explicit form for U is

$$U(\chi,R,0)=\frac{9A^{4/3}}{16\pi R_0^2}\theta(R-|\chi|/2)f(\chi/2R)\ , \tag{6.24}$$

where

$$f(\beta)=2(1-\beta^4)-\tfrac{4}{3}|\beta|(1-\beta^3)-(1-\beta^2)^2\ . \tag{6.25}$$

Note that the A dependence in U does not reside completely in the overall factor.

$\mathcal{S}^{2(a)}$ is an average over constituent nucleon momenta of an expression which, except for the geometrical factor $U(\xi_2^+/2\sqrt{2},R)$, would be a forward-scattering amplitude. We may note that in $\mathcal{S}^{2(b)}$ the gluon fields are anti-time-ordered,

$$\mathcal{S}^{2(b)}=-g^2(Q^2)\frac{l^+}{l^++q^+}\int d^4\xi_2\exp(-iq\cdot\xi_2)\int d^3\tilde{P}_2\bar{r}(P_2)\langle P_2|\bar{T}[v\cdot A^d(\xi_2/2)v\cdot A^d(-\xi_2/2)]|P_2\rangle$$
$$\times\theta(-\xi_2^+)U(\xi_2^+/2\sqrt{2},R,0)\ . \tag{6.26}$$

The hard factor in Eq. (6.20) is given by

$$\sigma_{2(a)}=\frac{C_F}{8}\frac{1}{l^+ +q^+}\int\frac{d^4p'}{(2\pi)^4}\frac{1}{6}\sum_m \mathrm{tr}[(\not{l}+\not{q})K_m^{2(a)*}\not{l}'H_m^{2(a)}]\int d^4\xi_1 e^{-ip'\cdot\xi_1}\int d^3\tilde{P}_1\bar{r}(P_1)\langle P_1|\phi_m^\dagger(\xi_1/2)\phi_m(-\xi_1/2)|P_1\rangle \ . \tag{6.27}$$

$\sigma_{2(a)}$ by itself is proportional to the cross section for the scattering of a quark of momentum $(l+q)^\mu$ with momentum transfer $(Q-q)^\mu$ by a nucleon of momentum P_1, averaged over P_1.

For comparison, $\sigma_{2(b)}$ is given by

$$\sigma_{2(b)}=\frac{C_F}{8}\frac{1}{l^+}\int\frac{d^4p'}{(2\pi)^4}\frac{1}{6}\sum_m \mathrm{tr}(\not{l}K_n^{*2(b)}\not{l}'H_m^{2(b)})\int d^4\xi_1 e^{-ip'\cdot\xi_1}\int d^3\tilde{P}_1\bar{r}(P_1)\langle P_1|\phi_m^\dagger(\xi_1/2)\phi_m(-\xi_1/2)|P_1\rangle \ . \tag{6.28}$$

K_m^* and H_m are ultraviolet coefficient functions, and to define them beyond lowest order requires a specific factorization scheme. To lowest order, however, they are given by the Born approximation. To this order, σ becomes a momentum-averaged elastic parton-hadron cross section of the parton model,

$$\begin{aligned}\sigma_{2(a)}&=\frac{C_F}{8}\int d^3P_1\bar{r}(P_1)\int_0^1 dx_m f_{m/N}(x_m)2\omega_{l'}\frac{d\sigma}{d^3l'}(x_m\hat{p}_1,l+q;l')\ ,\\ \sigma_{2(b)}&=\frac{C_F}{8}\int d^3P_1\bar{r}(P_1)\int_0^1 dx_m f_{m/N}(x_m)2\omega_{l'}\frac{d\sigma}{d^3l'}(x_m\hat{p}_1,l;l')\ ,\end{aligned} \tag{6.29}$$

where $d^3P_1\equiv d^2P_{1,\perp}dP_1^-$. Here $f_{m/N}(x_m)$ is the distribution of parton m in hadron N and $d\sigma(x_m\hat{p}_1,k,k')$ describes the process

$$\mathrm{quark}(k)+\mathrm{parton}(x_m\hat{p}_1)\rightarrow\mathrm{quark}(k')+X \ , \tag{6.30}$$

where

$$\hat{p}_1^\mu=\frac{1}{\sqrt{2}}[(\mathbf{P}_1^2+\mathrm{m}_N^2)^{1/2}+|\mathbf{P}_1|]\delta^{\mu-} \ , \tag{6.31}$$

and where the final parton is on-shell.

The contributions of Figs. 3 and 4 follow the same pattern. $\mathcal{S}^{3(a),3(b)}$ differs from $\mathcal{S}^{2(a),2(b)}$ only by overall kinematic factors,

$$\begin{aligned}\mathcal{S}^{3(a)}&=\left[\frac{l^+ +q^+}{l^+}\right]\left[\frac{(u'\cdot l')}{l'^+ -q^+}\right]^2\mathcal{S}^{2(a)}(v',q_{3(a)})\ ,\\ 2\,\mathrm{Re}\mathcal{S}^{3(b)}&=\left[\frac{l^+ +q^+}{l^+}\right]\left[\frac{(u'\cdot l)^2}{(l'-q^+)l'^+}\right]2\,\mathrm{Re}\mathcal{S}^{2(b)}(v',q_{3(b)})\ ,\end{aligned} \tag{6.32}$$

where the arguments on the right-hand side indicate necessary replacements. Note that the geometrical factor U, Eq. (6.25), is numerically the same as in Fig. 2. The hard parts are also of the same functional form

$$\begin{aligned}\sigma_{3(a)}&=\frac{C_F}{8}\int d^3P_1\bar{r}(P_1)\int_0^1 dx_m f_{m/N}(x_m)2\omega_{l'}\frac{d^3\sigma}{d^3l'}(l,x_m\hat{p}_1;l'-q)\ ,\\ \sigma_{3(b)}&=\frac{C_F}{8}\int d^3P_1\bar{r}(P_1)\int_0^1 dx_m f_{m/N}(x_m)2\omega_{l'}\frac{d^3\sigma}{d^3l'}(l,x_m\hat{p}_1;l')\ .\end{aligned} \tag{6.33}$$

The mixed-state graphs, Fig. 4, give related results for the soft factors,

$$\begin{aligned}\mathcal{S}^{4(a)}(p',q,k^-)&=g^2(Q^2)\frac{(u'\cdot l')}{l'^+ -q^+}\int d^4\xi_2 e^{-i(q-k^-/2u)\cdot\xi_2}\int d^3\tilde{P}_2\bar{r}(P_2)\langle P_2|v'\cdot A^d(\xi_2/2)v\cdot A^d(-\xi_2/2)|P_2\rangle\\ &\quad\times\theta(\xi_2^+)V(\xi_2^+/2\sqrt{2},R,k^-)\ ,\\ \mathcal{S}^{4(b)}(p',q,k^-)&=-g^2(Q^2)\frac{l^+(u'\cdot l')}{(l^+ -q^+)(l'^+ -q^+)}\int d^4\xi_2 e^{-i(q-k^-/2u)\cdot\xi_2}\int d^3\tilde{P}_2\bar{r}(P_2)\\ &\quad\times\langle P_2|\bar{T}(v'\cdot A^d(\xi_2/2)v\cdot A^d(-\xi_2/2))|P_2\rangle\\ &\quad\times\theta(\xi_2^+)V(\xi_2^+/2\sqrt{2},R,k^-)\ ,\end{aligned} \tag{6.34}$$

where

$$V(\chi,R,k^-)=\frac{9}{16\pi^2R_0^6}\int d^3y\,\rho(\mathbf{y})\int_{-|\chi|}^{|\chi|}d\alpha\,e^{+i\sqrt{2}k^-\alpha}\rho(\mathbf{y}+\alpha\mathbf{n})\ . \tag{6.35}$$

Note that, unlike U Eq. (6.23), V does not vanish for $|x|>R$. In fact, for $|\chi|>R$ and $k^-=0$, we have

$$V(\chi>R,R,0)=\frac{9A^{4/3}}{16\pi R_0^2}\ . \tag{6.36}$$

The short-distance functions are a bit more complicated than for Figs. 2 and 3 because for $q^\mu\neq 0$ they do not describe squared matrix elements. At lowest order, however, their hard scatterings are still given by the Born approximation and we may write

$$\sigma_{4(a)}=\tfrac{1}{8}\int d^3P_1\bar{r}(P_1)\int_0^1 dx_m f_{m/N}(x_m)\frac{1}{4(l^++q^+)x_mP_1^-}\sum T_bM^*(x_m\hat{p}_1+\hat{k},l;l'+\hat{k}-q)$$
$$\times\frac{1}{2(2\pi)^2}\delta((l+x_m\hat{p}_1-l'+q)^2)T_b'M(x_m\hat{p}_1,l+q;l')\ , \tag{6.37}$$
$$\sigma_{4(b)}=\tfrac{1}{8}\int d^3P_1\bar{r}(P_1)\int_0^1 dx_m f_{m/N}(x_m)\frac{1}{4l^+x_mP_1^-}\sum T_bM^*(x_m\hat{p}_1+\hat{k},l-q;l'+\hat{k}-q)$$
$$\times\frac{1}{2(2\pi)^2}\delta((l+x_m\hat{p}_1-l')^2)T_b'M(x_m\hat{p}_1,l;l')\ ,$$

where M is the Born approximation to the transition matrix. T_b and T_b' are color generators in the representations of the projectile and observed partons, respectively. $\sum$ indicates appropriate sums and averages over helicities and colors of these partons. In the $q^\mu=0$ limit, of course, these expressions do become parton-model cross sections.

In the following sections, we will show how the double scattering and interference terms for each diagram combine to suggest a gauge-invariant factorization of soft and hard contributions to the cross section.

VII. EXPANSION IN SOFT MOMENTA

Equation (6.20) gives the soft cross section in a partially factored form. It has, however, two drawbacks. First, the soft and hard factors are still linked by the q^+ and $\mathbf{q}_\perp$ integrals, and second, the matrix elements in the soft factor involve the gluon field, and hence are not gauge invariant. In this section, we shall address these limitations, showing how an expansion of the hard factor about $q^+=\mathbf{q}_\perp=0$ leads to a fully factorized form, in which the soft factor involves field strengths. This corresponds to eliminating longitudinal degrees of freedom in the soft scattering, as mentioned in Sec. III. Although the non-Abelian field strengths are gauge covariant, rather than invariant, enforcing gauge invariance requires only terms which are higher order in $\alpha_s(Q^2)$.

We may begin with the variable q^+. Since the expansion about $q^+=0$ must be boost invariant, it will be in terms of powers like $q^+/l^+\sim q^+/Q^+=O(mq^+/s)$. We therefore need consider only first order in q^+, since higher orders are suppressed by two powers of s. We can now show, however, that terms linear in q^+ are themselves suppressed from $O(s^{-1})$ to at least $O(s^{-3/2})$ by virtue of the Ward identity, Eq. (6.7). This is because the leading term in each of the projectile tensors is proportional to $v^\mu=\delta^{\mu+}$ and $v'^\mu=\delta^{\mu+}+O(Q_T/l^+)=\delta^{\mu+}+O(m/s^{1/2})$. In each case also, the index μ is contracted with a field operator in one of the matrix elements of Eqs. (5.21) or (5.22). Thus, we always have for terms linear in q^+ the combination

$$\frac{q^+}{l^+}[A^-(x)+R]=\frac{1}{l^+}[q^\mu A_\mu(x)-q^-A^+(x)$$
$$+\mathbf{q}_\perp\cdot\mathbf{A}_\perp(x)]\ , \tag{7.1}$$

where $R=0$ if $A(x)$ is contracted with v^μ, and $R=O(s^{-1/2})$ if with v'^μ. The first term on the right-hand side of Eq. (7.1) gives zero by (6.7). The second term is suppressed by at least an extra factor of $Q_\perp/l'^+\sim m/s^{1/2}$ by Eq. (6.21). Finally, the third term vanishes under symmetric integration at this order, and can only contribute if the hard part is also expanded about $q_\perp=0$, which will cost at least an extra factor of order $|\mathbf{q}_\perp|/|\mathbf{Q}_\perp|=O(s^{-1/2})$. In summary, the complete contribution of terms proportional to q^+ is suppressed by at least $s^{-3/2}$, and may thus be dropped in our approximation. This leaves us with only an expansion in $\mathbf{q}_\perp$. As observed above, terms proportional to $\mathbf{q}_\perp$ alone vanish, so that the first nonzero terms appear at order $\mathbf{q}_\perp^2/Q^2\sim\mathbf{q}_\perp^2/s$. Higher orders in $\mathbf{q}_\perp^2$ can be dropped since they are suppressed by further powers of s.

Once we drop the q^+ dependence in the σ_i (and in overall factors in the $\mathcal{S}^{(i)}$), the q^+ integral produces a factor $2\pi\delta(\xi_2^-)$. This, in turn, leads to a simplification for $\mathcal{S}^{i(b)}$, since with $\xi_2^-=0$, an ordering in ξ_2^+ is the same as an ordering in time. For instance, using the fact that $\sigma_{2(b)}$ and $\sigma_{2(a)}$ are real, the relevant real part in (6.20) with $i=2$ is

$$2\,\mathrm{Re}\int_{-\infty}^{\infty}\frac{dq^+}{2\pi}\mathcal{S}^{2(b)}=-2g^2\mathrm{Re}\int d^4\xi_2 e^{-i\hat{q}_2\cdot\xi_2}\int d^3\tilde{P}_2\bar{r}(P_2)\delta(\xi_2^-)$$
$$\times\theta(-\xi_2^+)\left\langle P_2\left|v\cdot A\left[\frac{\xi_2}{2}\right]v\cdot A\left[-\frac{\xi_2}{2}\right]\right|P_2\right\rangle U(\xi^+/2\sqrt{2},R,0)\ , \tag{7.2}$$

where we have used (6.26) and where we define [see Eq. (6.21)],

$$\hat{q}_2^\mu=(0^+,q_{2(a)},\mathbf{q}_\perp)\ . \tag{7.3}$$

Elementary manipulations then give the equality

$$-2\,\mathrm{Re}\int_{-\infty}^{\infty}\frac{dq^+}{2\pi}\mathcal{S}^{2(b)}=\int_{-\infty}^{\infty}\frac{dq^+}{2\pi}\mathcal{S}^{2(a)}\equiv E(q_\perp)\ , \tag{7.4}$$

where we note that $\hat{q}_2^{\,\mu}$ is a function of $q_\perp$. Now, combining (7.4) with Eq. (6.20) we find

$$2\omega_{l'}\frac{d\sigma_{\mathrm{soft}}^{(2)}}{d^3l'}=\int_\Sigma\frac{d^2q_\perp}{(2\pi)^2}E(q_\perp)$$
$$\times[\sigma_{2(a)}(l,l',\hat{q}_2)-\sigma_{2(b)}(l,l')]\ . \tag{7.5}$$

Since $\sigma_{2(a)}$ is a short-distance function, we may expand it about $\mathbf{q}_\perp=0$ in powers of $q_\perp^2/s$. Keeping, in accordance with our basic approximation, only the first-order term in this expansion, we find simply

$$2\omega_{l'}\frac{d\sigma_{\mathrm{soft}}^{(2)}}{d^3l'}=\frac{A^{4/3}}{R_0^2}IC_i\ ,$$
$$I(Q^2,R)=\frac{R_0^6}{R^4}\int_\Sigma\frac{d^2q_\perp}{(2\pi)^2}q_\perp^2E(q_\perp)\ , \tag{7.6}$$
$$C_i(Q^2)=\tfrac{1}{4}\sum_{i=1}^{2}\frac{d^2}{dq_i^2}\sigma_{2a}(p',l,l',\hat{q}_2)\Big|_{q_\perp=0}\ .$$

We have used the facts that E can only be a function of $|\mathbf{q}_\perp|$, and that $\sigma_{2(a)}(\hat{q}_2=0)=\sigma_{2(b)}$. C_i behaves as $Q_\perp^{-6}$, as compared to the $Q_\perp^{-4}$ of each term individually. Thus, as promised, the leading twist cancels. At this point, we can make the connection to the gluonic field strength anticipated in Sec. III. To do so, we notice that $q_\perp v\cdot A^a$ is one term in the Fourier transform of the contraction $v_\mu F^{\mu va}$. The other terms are q^-A^{va}, q^+A^-, and $C_{abc}g(Q^2)v\cdot A^bA^{vc}$. Of these, the first is higher order in $q_\perp$, since $q^-=q_\perp^2/2l^+$, the second is proportional to q^+ and hence suppressed by Ward identities, and the third is higher order in the effective coupling. Thus, to the order at which we work, we may make the replacement

$$q_\perp v\cdot A^d\left[\frac{\xi_2}{2}\right]q_\perp v\cdot A^d\left[-\frac{\xi_2}{2}\right]\to F^{-\mu d}(\xi_2/2)F_\mu^{-d}(-\xi_2/2) \tag{7.7}$$

in $q_\perp^2E(q_\perp)$, so that

$$I=g^2(Q^2)\int\frac{d^2q_\perp}{(2\pi)^2}\int d^4\xi_2\delta(\xi_2^-)e^{-i\hat{q}_2\cdot\xi_2}\int d^3\tilde{P}_2\bar{r}(P_2)\langle P_2|F^{-\mu d}(\xi_2/2)F_\mu^{-d}(-\xi_2/2)|P_2\rangle u(\xi_2^+/2\sqrt{2},R)\ ,$$
$$u(\chi,R)\equiv\frac{9}{16\pi^2R^4}\int d^3y\,\rho(\mathbf{y})\int_{-\infty}^{-|\chi|}d\alpha\,\rho(\mathbf{y}+\alpha\mathbf{n})\ . \tag{7.8}$$

This is the connection to gauge-covariant matrix elements anticipated above.

We can give a more physical interpretation to Eq. (7.8), by introducing the distribution of gluons at fixed-momentum fraction x *and* fixed transverse momentum $q_\perp$. This is given for a free hadron h by[22]

$$\mathcal{D}_{g/h}(x,q_\perp)=\frac{1}{xP^-}\int\frac{d\xi^+d^2\xi_\perp}{(2\pi)^3}e^{-ixP^-\xi^++i\mathbf{q}_\perp\cdot\xi_\perp}\langle P|F^{-\mu d}(\xi/2)F_\mu^{-d}(-\xi/2)|P\rangle\ . \tag{7.9}$$

From (7.9), Eq. (7.8) may be rewritten as

$$I=4\pi^2\alpha_s(Q^2)\int d^3P\,\bar{r}(P)P^-$$
$$\times\int d^2q_\perp\int_{-1}^{1}dx\,x\mathcal{D}_{g/N}(x,q_\perp)$$
$$\times\tilde{u}(q_\perp^+/2l^+-xP^-,R)\ , \tag{7.10}$$

where, once again, $d^3P=d^2P_\perp dP^-$, and where $\tilde{u}$ is the Fourier transform of u with respect to ξ_2^+

$$\tilde{u}(l^-,R)=\int\frac{d\xi^+}{2\pi}e^{-i\xi^+l^-}u(\xi^+/2\sqrt{2},R)\ . \tag{7.11}$$

Finally, we note the following relation,[22] which holds to leading-logarithm approximation:

$$xf_{g/N}(x,Q^2)=\int_{q_T^2<Q^2}d^2q_\perp\mathcal{D}_{g/N}(x,q_\perp)\ , \tag{7.12}$$

where $f_{g/N}(x,Q^2)$ is the distribution of gluons in the nu-

cleon at momentum fraction x. The precise upper limit in (7.12) is set by our choice of Σ_i in Eq. (4.2), which we now see has the usual interpretation of a factorization scale.[21] We cannot apply Eq. (7.12) to the $q_\perp$ integral of Eq. (7.10) as it stands, because $\tilde{u}$ depends on $q_\perp$. We may note, however, that if we expand $\tilde{u}(q_\perp^2/2l^+ - xP^-)$ about $q_\perp^2=0$, the first-order term is proportional to $A^{1/3}(l^+)^{-1}$ relative to the zeroth order, which is already suppressed to $O(Q_\perp^{-6})$. Such contributions we have agreed to neglect, so we find to this order that we can rewrite I in (7.6) as

$$I(Q^2,R)=8\pi^2\alpha_s(Q^2)\int d^3P\,\bar{r}(P)P^- \times\int_0^1 dx\, xf_{g/N}(x,Q^2) \times\tilde{u}(-xP^-,R)\,, \tag{7.13}$$

where we have used the fact[22] that $xf_{g/N}(x)$ is even in x, as is $\tilde{u}(-xP^-)$.

We should note here that $f_{g/N}$ in (7.13) is observable independently of $\bar{r}(P)$ only to the extent that we neglect interactions between nucleons. If we do, however, $f_{g/N}$ may be identified with the free nucleon distribution.

It is convenient now to consider the analogous reasoning for the graphs of Fig. 4. There are a number of differences in both the soft and hard contributions, which require a slightly different approach, and lead to slightly different results.

We begin by formally expanding the short-distance parts of (6.20) with $i=4$ about $\hat{q}^\mu=0$. Using Eq. (6.34), we find that adding the mirror diagrams of Figs. 4(a) and 4(b) has the effect of replacing $\theta(\xi_2^+)\theta(\frac{1}{2}\xi_2^+-|\eta|)$ by $\theta(\frac{1}{2}|\xi_2^+|-|\eta|)$, so that, for $\gamma=a$ or b,

$$2\,\mathrm{Re}\int\frac{dq^+d^2q_\perp}{(2\pi)^3}\mathcal{S}^{(4\gamma)}\sigma_{4\gamma}=\pm g^2(Q^2)\frac{u'\cdot l}{l'^+}\int\frac{d^2q_\perp}{(2\pi)^2}\int d^4\xi_2\,\delta(\xi_2^-)V\left[\frac{\xi_2^+}{2\sqrt{2}},R,\pm\frac{q_\perp^2}{2l^+}+\frac{-2Q_\perp\cdot q_\perp+q_\perp^2}{2l'^+}\right] \times\exp\left[i\mathbf{q}_\perp\cdot\boldsymbol{\xi}_{2\perp}\mp i\xi_2^+\frac{q_\perp^2}{4l^+}+i\xi_2^+\left[\frac{-2\mathbf{Q}_\perp\cdot\mathbf{q}_\perp+\mathbf{q}_\perp^2}{4l'^+}\right]\right] \times\int d^3\tilde{P}_2\bar{r}(P_2)\langle P_2|v'\cdot A^d(\tfrac{1}{2}\xi_2)v\cdot A^d(-\tfrac{1}{2}\xi_2)|P_2\rangle \times\left[\sigma_{4\gamma}(q_\perp=0)+q_i\left[\frac{d}{dq_i}\sigma_{4\gamma}\Big|_{q_\perp=0}\right]+\tfrac{1}{2}q_iq_j\left[\frac{d^2}{dq_idq_j}\sigma_{4\gamma}\Big|_{q_\perp=0}\right]\right], \tag{7.14}$$

where $i,j=1,2$. Here the upper sign refers to $\gamma=a$, the lower to $\gamma=b$. The only property of the expansion of $\sigma_{4\gamma}$ which we will need is that each derivative results in a suppression by $O(s^{-1/2})$. We shall refer to the term in (7.14) with n powers of q_i as $\tau_{4\gamma}^{(n)}$.

The essential difference between Figs. 2 and 4 is that V, Eq. (6.35), does not vanish for $(\frac{1}{4}\sqrt{2})|\xi_2^+|>R$. We must therefore be careful in expanding exponentials whose arguments include ξ_2^+. To handle this problem, we proceed as follows.

We divide the ξ_2^+ integral into two regions, (i) $|\xi_2^+|<4l^+/q_\perp^2$ and (ii) $|\xi_2^+|>4l^+/q_\perp^2$. In region (i), we may safely expand $\exp[\pm i\frac{1}{2}\xi_2^+(q_\perp^2/2l^+)]$, and our treatment is relatively straightforward. Region (ii) is potentially troublesome, but we can easily show that it can be ignored. Consider, for instance, the contribution to $\sigma_{4a}^{(0)}$ from (ii). If we define a new variable $\rho=q_\perp^2\xi^+/4l^+$ [$\rho\geq 1$ in region (ii)], we have

$$\tau_{4(a)}^{(0)}(\mathrm{ii})=g^2(Q^2)\frac{u'\cdot l}{l'^+}\int_\Sigma\frac{d^2q_\perp}{(2\pi)^2}\int d^2\xi_\perp e^{iq_\perp\xi_{2,\perp}} \times\frac{4l^+}{q_\perp^2}\int_1^\infty d\rho\,V\left[\frac{\sqrt{2}l^+\rho}{q_\perp^2},R,+\frac{q_\perp^2}{2l^+}+\frac{-2\mathbf{Q}_\perp\mathbf{q}_\perp+\mathbf{q}_\perp^2}{2l'^+}\right] \times\exp[-i\rho(1-l^+/l'^+)-i\rho(2\mathbf{Q}_\perp\cdot\mathbf{q}_\perp)/\mathbf{q}_\perp^2] \times\int d^3\tilde{P}_2\bar{r}(P_2)\langle P_2|v'\cdot A^d(\xi_2/2)v\cdot A^d(-\xi_2/2)|P_2\rangle\sigma_{4\gamma}(q_\perp=0)\,. \tag{7.15}$$

In this term, we see an essential singularity at $q_\perp=0$. This results in an exponential suppression like $e^{-|Q_{2\perp}|/|q_\perp|}$ of the low-$q_\perp$ region, as can most easily be seen by changing to polar coordinates and making appropriate deformations in the integration contours. Region (ii) does not contribute at all to an expansion in q_T/Q_T (which is incidentally an asymptotic expansion). As a consequence, all contributions to the expansion of each $\tau_{4\gamma}^{(m)}$ are from region (i), where we can expand exponentials of $(q^2/4l^+)\xi_2^+$, since this argument never exceeds unity. With this in mind, we may treat the cases $m=0$, 1, and 2 in turn.

For $m=0$, we first note that by Eqs. (6.27) and (6.28), $\sigma_{4(a)}(q=0)=\sigma_{4(b)}(q=0)$, so that

$$\tau^{(0)}_{4(a)}+\tau^{(0)}_{4(b)}=g^2(Q^2)\frac{u'\cdot l}{l'^+}\int\frac{d^2q_\perp}{(2\pi)^2}\int d^4\xi_2\delta(\xi_2^-)e^{iq_\perp\cdot\xi_{2\perp}}$$
$$\times\frac{9}{16\pi^2R_0^6}\int d\eta\, d^3y\,\rho(\mathbf{y})\rho(\mathbf{y}+(\eta/\sqrt{2})\mathbf{n})$$
$$\times\theta(|\xi_2^+/2|-|\eta|)\exp\left[i\left[\frac{-2Q_\perp\cdot q_\perp+q_\perp^2}{2l'^+}\right](\eta+\tfrac{1}{2}\xi_2^+)\right]$$
$$\times 2i\sin\left[\frac{q_\perp^2}{2l^+}(\eta-\tfrac{1}{2}\xi_2^+)\right]$$
$$\times\int d^3\tilde{P}_2\tilde{r}(P_2)\langle P_2|v'\cdot A^d(\tfrac{1}{2}\xi_2)v\cdot A^d(-\tfrac{1}{2}\xi_2)|P_2\rangle\sigma_{4(a)}(0)\ . \quad (7.16)$$

In region (i), the sine function is associated with a $q_\perp^2/l^+\sim q_\perp^2/Q^2$ suppression. This is the power we are after, and if we can show a further suppression, (7.16) will be negligible. In our approximation, we may replace v'^μ by v^μ in the matrix element, since the vectors differ only in components suppressed by a power of l^+. After this replacement, the matrix element becomes symmetric under the replacement $\xi_2^\mu\to-\xi^\mu$. This is because, with $\xi_2^-=0$, ξ^μ is either a spacelike ($\xi_{2\perp}\neq0$) or lightlike ($\xi_{2\perp}=0$) vector. For spacelike ξ_2^μ, $v\cdot A(\frac{1}{2}\xi_2)$ and $v\cdot A(-\frac{1}{2}\xi_2)$ certainly commute. In *connected* matrix elements—as all of ours are—these operators effectively commute on the light cone as well.[22,12,7] Now, once we know that the matrix element in (7.16) is even in ξ_2^μ, we can make the change of variables

$$q_\perp\to-q_\perp,\quad \xi^\mu\to-\xi^\mu,\quad \eta\to-\eta\ . \quad (7.17)$$

We easily see, again because of the sine, that (7.16) is odd under the transformation (7.17), and hence vanishes at this power.

We may now turn to the single derivative terms in Eq. (7.14). Noting that $(d/dq_i)\sigma_{4_\gamma}|_{q=0}$ is already suppressed by $O(1/Q_\perp)$, we may drop exponential $q_\perp^2/l^+$ dependence in $\tau^{(1)}_{4(a)}$ and $\tau^{(1)}_{4(b)}$, since this dependence is suppressed by $O(1/Q_\perp^3)$ compared to the leading term. Once this is done, it is easy to check that the remaining expressions for $\tau^{(1)}_{4(a)}$ and $\tau^{(1)}_{4(b)}$ are both odd under the same change of variables, Eq. (7.17), which we applied to $\tau^{(0)}_{4(a)}+\tau^{(0)}_{4(b)}$. As a result, the single-derivative terms may also be neglected.

These considerations leave only the second-derivative terms $\tau^{(2)}_{4(a)}$ and $\tau^{(2)}_{4(b)}$ in Eq. (7.14), which may still contribute at $O(1/Q_\perp^2)$ relative to leading behavior. The factors $(d^2/dq_i dq_j)\sigma_{4\gamma}|_{q=0}$ are already at this order, so once again we may neglect the $q_\perp^2/l^+$ terms in the exponentials. Then, using

$$\int_0^{2\pi}d\theta\, e^{-iz\cos\theta}\cos\theta\sin\theta=0\ , \quad (7.18)$$

we may make the same replacement $q_iq_j\to\frac{1}{2}q_i^2\delta_{ij}$ that we made for Fig. 2 in deriving Eq. (7.6). As a result, we will once again find field-strength matrix elements. From Eqs. (7.14) and (6.20), we have

$$\omega_{l'}\frac{d\sigma^{(4)}_{\rm soft}}{d^3l'}=\frac{A^{4/3}}{R_0^2}KB\ ,$$
$$K(Q^2,\hat{s},R)=g^2(Q^2)\int d\xi_2^+d^2\xi_{2,\perp}\int\frac{d^2q_\perp}{(2\pi)^2}\exp\left[-i\xi_2^+\frac{\mathbf{Q}_\perp\cdot\mathbf{q}_\perp}{2l'^+}+i\mathbf{q}_\perp\cdot\xi_{2,\perp}\right]\frac{R_0^6}{R^4}V\left[\frac{\xi_2^+}{2\sqrt{2}},R,-\frac{\mathbf{Q}_\perp\cdot\mathbf{q}_\perp}{l'^+}\right]$$
$$\times\int d^3P_2\tilde{r}(P_2)\langle P_2|F_\mu^{-d}(\tfrac{1}{2}\xi_2)F^{\mu-d}(-\tfrac{1}{2}\xi_2)|P_2\rangle\ , \quad (7.19)$$
$$B(Q^2)=\frac{1}{4}\left[\sum_{i=1}^2\frac{d^2}{dq_i^2}[\sigma_{4(a)}(\hat{q}_{4(a)})-\sigma_{4(b)}(\hat{q}_{4(b)})]\right]_{q=0}\ ,$$

where $\hat{s}\equiv\sqrt{2}l^+m$, with m the nucleon mass. $\sigma_{4(a),4(b)}$ is given by Eq. (6.37) with $\hat{q}^\mu_{4(a),4(b)}=(0^+,q_{4(a),4(b)},\mathbf{q}_\perp)$, where $q_{4(a),4(b)}$ is given in Eq. (6.21). Here we have used the fact that once the $q_\perp^2/l^+$ terms are neglected in exponentials, the soft factors in $\tau^{(2)}_{4(a)}$ and $\tau^{(2)}_{4(b)}$ become equal. $K(Q^2,\hat{s})$ differs from I, Eq. (7.8) only in that the density function V Eq. (6.35) has replaced U, Eq. (6.24), and in the values of q^- and k^-. So, in place of Eq. (7.10) we find

$$K=4\pi^2\alpha_s(Q^2)\int d^3P\,\tilde{r}(P)P^-\int d^2q_\perp\int_{-1}^1dx\,x\mathcal{D}_{g/N}(x,q_\perp)\frac{R_0^6}{R^4}\tilde{V}\left[\frac{\mathbf{Q}_\perp\cdot\mathbf{q}_\perp}{2l'^+}-xP^-,R,\frac{-\mathbf{Q}_\perp\cdot\mathbf{q}_\perp}{l'^+}\right]\ , \quad (7.20)$$

where $\tilde{V}$ is defined by analogy to $\tilde{u}$, Eq. (7.11).

To relate $d\sigma^{(4)}_{\rm soft}$ to the gluon distribution, we use the fact that, by comparing Eqs. (6.24) and (6.35), we can relate V to U. This comparison is made easier if we realize that $k^- \sim \mathbf{Q}_\perp \cdot \mathbf{q}_\perp / l^+$ may be neglected in V, since it is multipled by α, whose limits are set by R. Higher orders in $\mathbf{Q}_\perp \cdot \mathbf{q}_\perp \alpha / l^+$ are suppressed by at least an extra $(l^+)^{-1}$. With k^- set to zero we easily find

$$\frac{R_0^6}{R^4}\tilde{V}(z,R,0)=v\delta(z)-2\tilde{u}(z,R)\ ,$$
$$v=\frac{9}{16\pi^2R^4}\int d^3y\int_{-\infty}^{\infty}d\alpha\,\rho(\mathbf{y})\rho(\mathbf{y}+\alpha\mathbf{n})\ . \tag{7.21}$$

For a spherical, homogeneous nucleus, $v=9/8\pi$. Substituted into (7.20), this in turn results in

$$K(Q^2,\hat{s},R)=4\pi^2\alpha_s(Q^2)v\int d^3P\,\bar{r}(P)\int d^2q_\perp\left[\frac{\mathbf{Q}_\perp\cdot\mathbf{q}_\perp}{2l'^+P^-}\right]\mathcal{D}_{g/N}\left[\frac{\mathbf{Q}_\perp\cdot\mathbf{q}_\perp}{2l'^+P^-},q_\perp\right]-2I$$
$$=J(Q^2,\hat{s},R)-2I(Q^2R)\ , \tag{7.22}$$

where I is given by (7.13) and where the second line is a definition of $J(Q^2,R)$.

Finally, for Fig. 3, the approximations developed above may be used to show that

$$2\omega_{l'}\frac{d\sigma}{d^3l'}=\frac{A^{4/3}}{R_0^2}IC_f\ , \tag{7.23}$$

where, again, I is given by (7.13), and where

$$C_f(Q^2)=\tfrac{1}{4}\sum_{i=1}^{2}\frac{d^3}{dq_i^2}\sigma_{3(a)}(\hat{q}_3)\Big|_{q_\perp=0}\ . \tag{7.24}$$

As usual $\hat{q}_3=(0^+,q_3,\mathbf{q}_\perp)$. In summary, we can combine Eqs. (7.6), (7.19), (7.22), and (7.23), for a complete form of the soft $O(A^{4/3}/R_0^2Q^2)$ correction to the cross section,

$$2\omega_{l'}\frac{d\sigma_{\rm soft}}{d^3l'}=\frac{A^{4/3}}{R_0^2}[I(C_i+C_f)+(J-2I)B] \tag{7.25}$$

with C_i, C_f, and B specified by (7.6) and (6.29), (7.24) and (6.33), and (7.19) and (6.37), respectively.

VIII. THE DOUBLE-SCATTERING CROSS SECTION

Having derived the soft-scattering cross section, Eq. (7.25), we can now combine it with the hard-scattering model of Sec. II, and exhibit a full double-scattering cross section. In doing so, we must be careful to avoid double counting and to pay attention to our approximations. The soft-scattering form, Eq. (7.25), has been derived under the assumption that $q_\perp^2$ is small compared to Q^2, and it fails for large $q_\perp$. Similarly the hard-scattering model, Eq. (2.5), fails for $q_\perp$ of order $\Lambda_{\rm QCD}$. To deal with the intermediate region, we can define an appropriate "subtraction" term,[7] which cancels redundant and inaccurate parts of $d\sigma_{\rm soft}$ and $d\sigma_{\rm hard}$. This term may be identified by noting that for $q_\perp \gg \Lambda_{\rm QCD}$, the soft cross sections $S^{(n)}$ with $n=2,3$ obey

$$S^{(n,a)}(k,k')=S^{(n,b)}(k,k')$$
$$=u(0,R)\frac{A^{4/3}}{R_0^2}\frac{h_t^{ii}(k,k')}{k'^+}\ , \tag{8.1}$$

where h_t^{ii} is the single particle inclusive cross section due to gluon exchange in the t channel, and is hence flavor diagonal. u is defined in Eq. (7.8), and for a spherical homogeneous nucleus, $u(0,R)=9/16\pi$.

Using Eq. (8.1), we find that $\omega_{l'}d\sigma^{(2)}_{\rm soft}/d^3l'+\omega_{l'}d\sigma^{(3)}_{\rm soft}/d^3l'$ is well approximated by

$$L^{ik}=\frac{A^{4/3}}{R_0^2}u(0,R)$$
$$\times\int\frac{dq^+d^2q_\perp}{l^++q^+}q_\perp^2[h_t^{ii}(l,l+q)C_i^{ik}+h_t^{ii}(l',l+q)C_f^{ik}]\ , \tag{8.2}$$

whenever $q_\perp^2 \gg \Lambda_{\rm QCD}$. But Eq. (8.2) can also be derived directly from Eq. (2.5) in the limit $q_\perp^2 \ll Q^2$ by neglecting higher-order terms in $q_\perp^2/Q^2$. As $|q_\perp|$ approaches $O(Q)$, however, $d\sigma_{\rm hard}$ will differ from Eq. (8.2) as these terms become important. In the combination $\omega_{l'}d\sigma^{(2)}_{\rm soft}/d^3l'+\omega_{l'}d\sigma^{(3)}_{\rm soft}/d^3l'+\omega_{l'}d\sigma_{\rm hard}/d^3l'-L$, L cancels $d\sigma_{\rm hard}$ where $d\sigma^{(2)}_{\rm soft}+d\sigma^{(3)}_{\rm soft}$ is appropriate and vice versa, while it cancels either in the overlap region $\Lambda_{\rm QCD}^2 \ll q_\perp^2 \ll Q^2$. To make $d\sigma_{\rm hard}$ formally comparable to $d\sigma_{\rm soft}$ we should replace the factor $(9/16\pi)$ in (2.5) by $u(0,R)$.

To get a complete formula for double scattering, we must add the contribution of Fig. 4, Eq. (7.19). These mixed-state interactions have no analog in the hard-scattering cross section, Eq. (2.5) so there is no problem with double counting here. Strictly speaking, to get the complete contribution of Fig. 4, we should use the form of Eq. (7.20) in which we have not expanded $\tilde{V}$ about $q_\perp=0$. The reason for this is that when $q_\perp=O(Q)$ the oscillations in V, Eq. (6.35), due to the factor $\exp[-i\sqrt{2}(\mathbf{Q}_\perp\cdot\mathbf{q}_\perp/l'^+)\eta]$ will cut off the $A^{4/3}$ behavior and return it to A^1. This, by the way, shows the self-consistency of the hard-scattering picture for $q_\perp=O(Q)$. Then the complete double-scattering cross section is

$$\omega_{l'}\frac{d\sigma^{ik}}{d^3l'}=\frac{A^{4/3}}{R_0^2}[I(C_i^{ik}+C_f^{ik})+KB^{ik}]+\omega_{l'}\frac{d\sigma^{ik}_{\rm hard}}{d^3l'}-L^{ik}\ , \tag{8.3}$$

where $d\sigma^{ik}_{\rm hard}$ is given by (2.5) and L^{ik} by (8.2). We can relate Eq. (8.3) more closely to the final form of $d\sigma_{\rm soft}$, Eq. (7.25), by noting that K Eq. (7.22) involves $\mathcal{D}_{g/N}(x,q_\perp)$ at $x=Q_\perp\cdot q_\perp/2l'^+P^-\sim k^-/P^-$. Now $\mathcal{D}_{g/N}(x,q_\perp)$ is expected to decrease rapidly as $x\to 1$. Thus, when k^- is large enough to make K decrease in $A^{1/3}$, it is also large enough to give a suppression in K via the gluon distribution. To a reasonable approximation, we may therefore replace the form (7.20) of K with (7.22) in the complete cross section. Equation (8.3) then becomes

$$\omega_{l'}\frac{d\sigma^{ik}}{d^3l'}=\frac{A^{4/3}}{p^2}[I(C_i^{ik}+C_f^{ik}-2B^{ik})+JB^{ik}] +\omega_{l'}\frac{d\sigma^{ik}_{\rm hard}}{d^3l'}-L^{ik}\ . \tag{8.4}$$

We have derived Eqs. (8.3) and (8.4) for jet or single-particle inclusive cross sections for hadrons. Nothing prevents us from applying it as well to leptonic cross sections such as deeply inelastic lepton production of jets or high-$P_\perp$ particles or the Drell-Yan process. In these cases only final- or initial-state corrections contribute, and Eq. (8.4) is considerably simplified.

Of special interest in Eq. (8.4) is the factor I, Eq. (7.14), which can be computed from the gluon distribution $f_{g/N}(x)$ and the density function $\rho(r)$ in Eq. (5.15). For leptonic processes this is the only nonperturbative factor. We can illustrate the nature of I, and its sensitivity to the low-x behavior of the gluon distribution by making the approximations

$$\rho(r)=\theta(R-r),\quad \tilde r(P)=\delta^3(P^- - m/\sqrt{2}) \tag{8.5}$$

appropriate to a homogeneous spherical nucleus in which we neglect Fermi motion. In this approximation,

$$P^-\tilde u(-xP^-,R)=\frac{9}{16\pi^2}\left[\left[1+\frac{2}{z^2}\frac{d^2}{dx^2} -\frac{5}{3}\frac{1}{z^4}\frac{d^4}{dx^4}\right]\frac{\sin zx}{x} +\frac{4}{3}\frac{1}{z^3}\frac{d^3}{dx^3}\frac{\sin\frac{1}{2}zx}{x}\right], \tag{8.6}$$

where

$$z\equiv 4mR\ . \tag{8.7}$$

Note that in the $R\to\infty$ limit, the function $(1/x)\sin zx$ acts like a δ function in x at $x=0$. For finite R, of course, it will simply emphasize the $x\to 0$ behavior of $xf_{g/N}(x)$ in

$$I=8\pi^2\alpha_s(Q^2)\int_0^1 dx\ xf_{g/N}(x)P^-\tilde u(-xP,R)\ , \tag{8.8}$$

where we have used (8.5) in (7.13). To be explicit, suppose we take the behavior[8]

$$xf_{g/N}(x)=\frac{c}{x^\Delta}g(x)\ , \tag{8.9}$$

where c is a constant and $g(x)$ is, typically, some polynomial in x with $g(0)=1$. Then it is not difficult to isolate the leading behavior in $A=R^3/R_0^3$ in (8.7),

$$I=c\frac{9\alpha_s}{2}(4mR_0A^{1/3})^\Delta\Gamma(1-\Delta) \times\left[\sin\frac{\Delta\pi}{2}\left[\frac{2+3\Delta}{\Delta(2+\Delta)}-\frac{5}{12+3\Delta}-\frac{4}{9+3\Delta}\right] -\frac{4}{9+3\Delta}\frac{1}{\Gamma(-2-\Delta)}\right]. \tag{8.10}$$

We see that the leading power in A, from I in (8.3), is directly dependent on Δ. [We note that K, Eq. (7.22) is independent of A for a homogeneous nucleus.] Whether Eq. (8.10), or a more sophisticated expression of this type, can actually be used to relate actual data to the gluon distribution is a natural question, which we leave for future work.

ACKNOWLEDGMENTS

The authors acknowledge very useful discussions with Fred Goldhaber, Robert McCarthy, Al Mueller, and Frank Paige. This work was supported in part by the National Science Foundation under Grants Nos. PHY-85-07627 and PHY-86-08418.

[1] J. W. Cronin *et al.*, Phys. Rev. D **11**, 3105 (1975); L. Kluberg *et al.*, Phys. Rev. Lett. **38**, 670 (1977); R. L. McCarthy *et al.*, *ibid.* **40**, 213 (1978); D. Antreasyan *et al.*, Phys. Rev. D **19**, 764 (1979); H. Jostlein *et al.*, *ibid.* **20**, 53 (1979); Y. B. Hsiung *et al.*, Phys. Rev. Lett. **55**, 457 (1985); K. Freudenreich, in *Proceedings of XXIII International Conference on High Energy Physics*, Berkeley, California, 1986, edited by S. Loken (World Scientific, Singapore, 1987).

[2] P. M. Fishbane and J. S. Trefil, Phys. Rev. D **12**, 2113 (1975); J. H. Kuhn, *ibid.* **13**, 2948 (1976); P. M. Fishbane, J. K. Kotsonis, and J. S. Trefil, *ibid.* **16**, 122 (1977); M. J. Longo, Nucl. Phys. **B134**, 70 (1978); V. V. Zmushko, Yad. Fiz. **32**, 246 (1980) [Sov. J. Nucl. Phys. **32**, 127 (1980)].

[3] A. Krzywicki, J. Engels, B. Petersson, and U. Sukhatme, Phys. Lett. **85B**, 407 (1979); M. Lev and B. Petersson, Z. Phys. C **21**, 155 (1983).

[4] K. Kastella, Phys. Rev. D **36**, 2734 (1987).

[5] G. Bodwin, S. J. Brodsky, and G. P. Lepage, Phys. Rev. Lett. **47**, 1799 (1981).

[6] W. W. Lindsay, D. A. Ross, and C. T. Sachrajda, Nucl. Phys. **B214**, 61 (1982).

[7] G. T. Bodwin, Phys. Rev. D **31**, 2616 (1985); J. C. Collins, D. E. Soper, and G. Sterman, Nucl. Phys. **B261**, 104 (1985); **B308**, 833 (1988).

[8] J. C. Collins, in Proceeding of 7th Topical Workshop on Proton-Antiproton Collider Physics, 1988 (unpublished).

[9]P. Chiappetta and H. J. Pirner, Nucl. Phys. **B291**, 765 (1987).
[10]H. D. Politzer, Nucl. Phys. **B172**, 349 (1980).
[11]R. L. Jaffe and M. Soldate, Phys. Lett. **105B**, 467 (1981); R. K. Ellis, W. Furmanski, and R. Petronzio, Nucl. Phys. **B212**, 29 (1983).
[12]R. L. Jaffe, Nucl. Phys. **B229**, 205 (1983).
[13]R. Doria, J. Frenkel, and J. C. Taylor, Nucl. Phys. **B168**, 93 (1980); C. Di'Lieto, S. Gendron, I. G. Halliday, and C. T. Sachrajda, *ibid.* **B183**, 223 (1981); F. T. Brandt, J. Frenkel, and J. C. Taylor, *ibid.* **B312**, 589 (1989).
[14]R. Basu, A. Ramalho, and G. Sterman, Nucl. Phys. **B244**, 221 (1984).
[15]J. H. Weiss, Acta Phys. Pol. **B7**, 851 (1976).
[16]S. Brodsky, G. P. Lepage, and P. Mackenzie, Phys. Rev. D **28**, 228 (1983); D. W. Duke and R. G. Roberts, Phys. Rep. **120**, 275 (1985).
[17]A. H. Mueller, in *Proceedings of the XVII Recontre de Moriond on Elementary Particle physics: II. Elementary Hadronic Processes and New Spectroscopy,* Les Arcs, France, 1982, edited by Tran Thanh Van (Edition Frontieres, Gif-sur-Yvette, France, 1982).
[18]S. Libby and G. Sterman, Phys. Rev. D **18**, 4737 (1978); J. M. F. Labastida and G. Sterman, Nucl. Phys. **B254**, 425 (1985).
[19]C. De Tar, S. D. Ellis, and P. V. Lanshoff, Nucl. Phys. **87**, 176 (1975); J. L. Cardy and G. A. Window, Phys. Lett. **52B**, 95 (1974).
[20]J. Qiu, Argonne Report No. ANL-HEP-PR-88-10 (unpublished).
[21]P. M. Stevenson and H. D. Politzer, Nucl. Phys. **B277**, 758 (1986).
[22]J. C. Collins and D. E. Soper, Nucl. Phys. **B194**, 445 (1982).